

# Embodied4C: Measuring What Matters for Embodied Vision-Language Navigation

Tin Stribor Sohn<sup>1,4†\*</sup> Maximilian Dillitzer<sup>2,4\*</sup> Can Kandil<sup>3,4\*</sup>

Jason J. Corso<sup>5,6</sup> Eric Sax<sup>1</sup>

<sup>1</sup> Karlsruhe Institute of Technology <sup>2</sup> UAS Esslingen <sup>3</sup> TU Wien

<sup>4</sup> Dr. Ing. h.c. F. Porsche AG <sup>5</sup> University of Michigan <sup>6</sup> Voxel51 Inc.

tin\_stribor.sohn@porsche.de

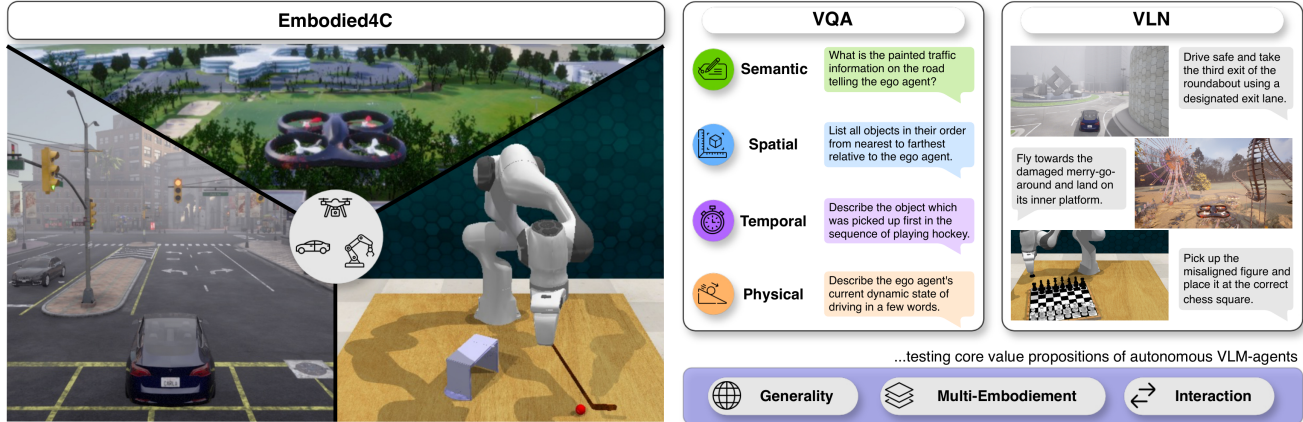


Figure 1. **Overview of the Embodied4C benchmark.** Embodied4C spans three embodiment domains (autonomous driving, aerial navigation, robotic manipulation) and four embodied scenario understanding capabilities (semantic, spatial, temporal, physical). The benchmark evaluates autonomous agents in visual question answering and vision-language navigation for scenario understanding and control execution, and includes domain-far questions to probe generalization (i.e., sensor set, general knowledge, weather, scenario). This design targets core value propositions of vision-language models as embodied agents: generality, multi-embodiment competence, and natural interaction.

## Abstract

*Vision-language navigation requires agents to reason and act under constraints of embodiment. While vision-language models (VLMs) demonstrate strong generalization, current benchmarks provide limited understanding of how embodiment—i.e., the choice of physical platform, sensor configuration, and modality alignment— influences perception, reasoning, and control. We introduce **Embodied4C**, a closed-loop benchmark designed as a Turing test for embodied reasoning. The benchmark evaluates the core embodied capabilities of VLMs across three heterogeneous embodiments—autonomous vehicles, aerial drones, and*

*robotic manipulators—through approximately 1.1K one-shot reasoning questions and 58 goal-directed navigation tasks. These tasks jointly assess four foundational dimensions: semantic, spatial, temporal, and physical reasoning. Each embodiment presents dynamic sensor configurations and environment variations to probe generalization beyond platform-specific adaptation. To prevent embodiment overfitting, Embodied4C integrates domain-far queries targeting abstract and cross-context reasoning. Comprehensive evaluation across ten state-of-the-art VLMs and four embodied control baselines shows that cross-modal alignment and instruction tuning matter more than scale, while spatial and temporal reasoning remains the primary bottleneck for reliable embodied competence.*

\*Equal contribution; †Corresponding author.

## 1. Introduction

Vision-language models (VLMs) are increasingly applied in autonomous systems to unify perception, reasoning, and control through a shared language-based interface [25, 30]. In vision-language navigation (VLN), this integration facilitates interpretable decision-making, open-ended instruction following, and context-aware behavior. Yet, existing evaluation practices rarely capture the core prerequisite for reliable performance in embodied environments: the capability for robust *scenario understanding*.

Scenario understanding encompasses the ability to represent and reason about a situation across four core dimensions: *semantic*, *spatial*, *temporal*, and *physical* understanding [74]. While existing benchmarks typically emphasize downstream task performance, they rarely isolate these foundational capabilities, making it difficult to attribute model behavior to specific reasoning deficits or strengths [73]. Furthermore, many benchmarks are susceptible to *inductive bias*: narrow task distributions, static sensor configurations, multiple-choice questioning, and fixed language templates allow models to overfit, yielding high scores without demonstrating true generalization [8, 102].

To address these limitations, we introduce **Embodied4C**, a closed-loop benchmark designed to evaluate the embodied reasoning capabilities of VLMs in visual question answering (VQA) and VLN. Conceptually, it serves as a *Turing test for embodied intelligence*, assessing whether models can exhibit human-like understanding when perception, language, and action are integrated. In contrast to prior work that is restricted to only one domain [24, 45, 73], our benchmark spans multiple embodiments—autonomous ground vehicles, unmanned aerial vehicles (UAVs), and robotic manipulators—to systematically assess embodiment sensitivity and generalization. Embodied4C probes the four aforementioned reasoning capabilities through two complementary tasks: (1) *VQA* to assess scenario understanding, and (2) *VLN* to evaluate control and decision-making in realistic simulation environments. Both tasks are conducted in a closed-loop setting, ensuring that model outputs have causal impact on the environment.

A central feature of the benchmark is its additional focus on the *value propositions of embodied agents* [56]. Specifically, the benchmark measures: (i) *Generality*, operationalized through domain-far queries, embodiment changes, and domain shifts; (ii) *Embodiment-awareness*, captured via varying sensor modalities, placements, and physical configurations; and (iii) *Interactivity*, realized through closed-loop evaluation of VQA and VLN where perception, reasoning, and control are tightly coupled. To our knowledge, Embodied4C is the first benchmark to explicitly probe these propositions alongside the four core reasoning capabilities. This work makes the following key contributions:

- We introduce Embodied4C, the first closed-loop bench-

mark framework that unifies evaluation of core VLM value propositions across heterogeneous embodiments, while systematically probing semantic, spatial, temporal, and physical reasoning capabilities.

- We develop a structured, exam-inspired, one-shot task design that operationalizes these evaluations through embodiment generalization, domain shifts, and domain-far reasoning challenges, mitigating overfitting and enabling granular attribution of embodied competencies.
- We provide a unified evaluation across three embodiment domains (ground vehicles, UAVs, robotic manipulators) to analyze the impact on perception, reasoning, and control on free-form VQA to reduce inductive answer biases.
- We conduct a comprehensive evaluation of ten pre-trained VLMs [1–3, 23, 38, 52, 54, 75] and four domain-specialized models [22, 34, 37, 39], demonstrating both strengths and limitations in scenario understanding and embodied autonomous navigation.

Embodied4C establishes a novel evaluation framework for measuring what matters in embodied VLN, supporting the development of robust, general-purpose autonomous agents. All code will be open sourced upon publication.

## 2. Related Work

Benchmarking in autonomous navigation has evolved from static dataset evaluations toward dynamic, task-oriented paradigms [85]. Early benchmarks primarily assessed perception or prediction in isolation, while recent approaches increasingly emphasize closed-loop evaluation, multimodal reasoning, and embodied interaction [24, 45, 73]. This section contrasts representative benchmarks along these dimensions, starting with driving-focused benchmarks and extending to embodied evaluation settings (cf. Table 1).

### 2.1. Driving Benchmarks

Recent benchmarks in autonomous driving have predominantly focused on semantic and spatial reasoning, while often neglecting temporal and physical understanding. Early works such as DriveMLM [25], SpatialRGPT [12], and NuScenes-based benchmarks [31, 59, 76] primarily target spatial perception, typically formulated as question answering (QA) on static scenes. Similarly, benchmarks like Talk2BEV [14], CODA-LM [9], MapLM [7], and Bench2ADVLM [98] extend to semantic querying but remain limited as Bench2ADVLM is the only to evaluate VLN. Other works such as NuPrompt [86], VLAAD [57], and LingoQA [51] incorporate temporal reasoning dimensions, but do not capture embodiment or physical interactions. More comprehensive efforts such as Reason2Drive [53], Rank2Tell [64], NuInstruct [16], and DriveBench [88] integrate temporal reasoning yet remain constrained to vehicle-based settings and lack embodiment

Benchmark	SEM	SPA	TEM	PHY	GEN	EMB	INT	VLN
DriveMLM [25]	✗	✓	✗	✗	✗	✗	✓	✗
SpatialRGPT [12]	✗	✓	✗	✗	✗	✗	✓	✗
NuScenes-MQA [31]	✗	✓	✗	✗	✗	✗	✓	✗
NuScenes-SpatialQA [76]	✗	✓	✗	✗	✗	✗	✓	✗
NuScenes-QA [59]	✓	✓	✗	✗	✗	✗	✓	✗
Talk2BEV [14]	✓	✓	✗	✗	✗	✗	✓	✗
CODA-LM [9]	✓	✓	✗	✗	✗	✗	✓	✗
MapLM [7]	✓	✓	✗	✗	✗	✗	✓	✗
Bench2ADVLM [98]	✓	✓	✗	✗	✓	✗	✓	✓
NuPrompt [86]	✓	✗	✓	✗	✗	✗	✗	✗
LingoQA [51]	✓	✗	✓	✗	✗	✗	✓	✗
VLAAD [57]	✓	✗	✓	✗	✗	✗	✓	✗
Reason2Drive [53]	✓	✓	✓	✗	✗	✗	✓	✗
Rank2Tell [64]	✓	✓	✓	✗	✗	✗	✓	✗
NuInstruct [16]	✓	✓	✓	✗	✗	✗	✓	✗
DriveBench [88]	✓	✓	✓	✗	✓	✗	✓	✗
VLADBench [44]	✓	✓	✓	✗	✓	✗	✓	✗
DriveLM [71]	✓	✓	✓	✗	✗	✗	✓	✓
DVBench [97]	✓	✓	✗	✓	✗	✗	✗	✗
Drive4C [73]	✓	✓	✓	✓	✗	✗	✓	✓
UAV-ON [87]	✓	✗	✗	✗	✓	✗	✗	✓
CityNav [40]	✓	✓	✗	✗	✓	✗	✗	✓
AerialVLN [45]	✓	✓	✗	✗	✓	✗	✗	✓
UAV-Need-Help [82]	✓	✓	✗	✗	✓	✗	✗	✓
EmbodiedCity [21]	✓	✓	✗	✗	✗	✗	✓	✓
AVDN [19]	✓	✓	✗	✗	✓	✗	✓	✓
OpenFly [22]	✓	✓	✗	✗	✓	✗	✓	✓
AeroVerse [94]	✓	✓	✗	✗	✓	✗	✓	✓
UAV3D [95]	✓	✓	✓	✗	✗	✗	✗	✗
ManipBench [101]	✓	✓	✗	✗	✗	✗	✗	✗
$\lambda$ [32]	✓	✓	✗	✗	✗	✗	✓	✓
SIMPLER [43]	✓	✓	✗	✗	✓	✗	✗	✓
VLMbench [103]	✓	✓	✗	✗	✓	✗	✗	✓
BulletArm [78]	✓	✓	✗	✗	✗	✓	✗	✓
RLBench [33]	✓	✓	✗	✗	✓	✓	✗	✓
EmbodiedEval [13]	✓	✓	✗	✗	✓	✗	✓	✓
EmbodiedBench [92]	✓	✓	✗	✗	✓	✗	✓	✓
BEHAVIOR-1K [41]	✓	✓	✗	✓	✓	✗	✗	✗
ARNOLD [24]	✓	✓	✗	✓	✓	✗	✗	✓
<b>Embodied4C (Ours)</b>	✓	✓	✓	✓	✓	✓	✓	✓

Table 1. **Overview of vision-language navigation benchmarks.** Columns “SEM”, “SPA”, “TEM”, and “PHY” indicate coverage of semantic, spatial, temporal, and physical understanding. “GEN”, “EMB”, “INT”, and “VLN” indicate the probing of key value propositions of autonomous agents: generality, multi-embodiment, interaction (i.e., VQA), and vision-language navigation.

generality. Extensions such as VLADBench [44], DriveLM [71], and DVBench [97] provide broader scene coverage and interaction, but embodiment and generality are not considered. Drive4C [73] is the first to systematically align driving evaluation with the four capability dimensions (semantic, spatial, temporal, physical) [74]. While Drive4C introduces a capability-driven evaluation, it lacks probing different embodiments and tasks related to the core value propositions of embodied agents.

## 2.2. UAV Benchmarks

In UAV navigation, most benchmarks inherently require semantic and spatial understanding, since tasks are typically

framed as following instructions such as “navigate to the red building” or “find the blue elephant”. Examples include UAV-ON [87], CityNav [40], AerialVLN [45], and UAV-Need-Help [82]. These benchmarks assess VLN but rarely integrate interaction capabilities such as VQA. UAV3D [95] adds a temporal dimension but remains confined to object detection and tracking in single and collaborative UAV formations, without evaluating key value propositions of VLMs. AVDN [19], EmbodiedCity [21], OpenFly [22], and AeroVerse [94] extend UAV navigation towards interactive scenarios. While EmbodiedCity and AeroVerse both claim to address multi embodiment, the current implementation of EmbodiedCity (as of November 2025) and the method of

AeroVerse remain specialized to aerial agents and do not by themselves evaluate multi-embodiment generality.

### 2.3. Manipulation Benchmarks

ManipBench [101] provides a large-scale multiple-choice evaluation, targeting diverse manipulation tasks. Instead of VQA-only, robotics manipulation benchmarks such as  $\lambda$  [32], SIMPLER [43], and VLMbench [103] are centered around VLN for task following, inherently probing semantic and spatial understanding. More advanced setups such as EmbodiedEval [13], EmbodiedBench [92], BEHAVIOR-1K [41], and ARNOLD [24] integrate larger task suites and either include interaction or partially address physical reasoning. BulletArm [78] and RLBench [33] explicitly consider embodiment by switching across different robotic arms, thereby going beyond single-agent manipulation. However, their embodiment remains limited to variations of robotic manipulators, without covering heterogeneous platforms such as ground vehicles or UAVs.

### 2.4. Summary

As summarized in Table 1, existing benchmarks either specialize in a single domain or probe only a subset of the required capabilities. None jointly address semantic, spatial, temporal, and physical reasoning while simultaneously evaluating generality, multi-embodiment, interaction, and VLN. Embodied4C fills this gap by providing the first unified capability-driven evaluation framework across heterogeneous embodiments, ranging from ground vehicles and UAVs to robotic manipulators.

## 3. The Embodied4C Benchmark

In this section, we present the **Embodied4C** benchmark, a closed-loop evaluation framework for assessing vision-language reasoning and control of autonomous agents across three domains: autonomous driving, aerial navigation, and robotic manipulation. In contrast to prior work that focuses on a single embodiment [43, 71, 73, 78, 82, 87], Embodied4C unifies these domains into a single benchmark, allowing cross-domain analysis of true embodiment.

### 3.1. Benchmark Structure

The benchmark probes four core embodied capabilities—semantic, spatial, temporal, and physical understanding—through non-templated VQA tasks, while VLN serves as a separate downstream category that unifies these capabilities in closed-loop control. Embodied4C comprises 1,149 unique, handcrafted VQA pairs, 13 sensor setups, and 58 VLN tasks across three simulation platforms, forming a deliberately heterogeneous testbed for systematic analysis of embodied agents. Evaluation is separated into two complementary task modalities:

- **VQA (interaction stage):** agents answer free-form, open-ended questions grounded in the environment. A reference agent navigates each scenario to ensure that all models under test are exposed to the same observations and related questions, thereby removing confounding effects of execution errors. In addition, sensor set and weather shifts, as well as domain-far questions are injected to probe generality beyond the task domain.

- **VLN (control stage):** agents follow natural language navigation or manipulation instructions and generate continuous control commands based on a provided action space (cf. Tables 7–9). Unlike VQA, VLN performance directly depends on how well embodied reasoning capabilities translate into closed-loop execution.

This design isolates scenario understanding (i.e., VQA) from control (i.e., VLN), while ensuring comparability across embodiments by defining a unified system prompt for all agents (cf. Table 4). Applying this high-level instruction structure to all agents similarly, avoids prompt-induced variability across all embodiments and models. Both, VQA and VLN, are evaluated within each of the three embodiment domains separately.

### 3.2. Probing Core Capabilities

Embodied4C probes four embodied reasoning capabilities:

- **Semantic:** reasoning about object categories, attributes, and contextual states.
- **Spatial:** reasoning about location, distance, orientation, topology, and qualitative relations.
- **Temporal:** reasoning about dynamics and temporal dependencies across short and long horizons.
- **Physical:** reasoning about physical models, dynamic constraints, and material properties.

Statistics regarding the distribution of question types across embodiments are reported in Appendix 6.1 (cf. Figure 3).

### 3.3. Embodiment Domains

Each domain provides a simulator environment with realistic dynamics:

- **Autonomous Driving** (CARLA [18, 73]): scenarios span highway, urban, suburban and rural settings, with variable traffic density and weather/illumination perturbations. Agents receive multimodal vehicle-mounted sensor streams and are evaluated on VQA along reference trajectories, followed by VLN driving tasks (e.g., “turn left at the next intersection”).
- **Aerial Navigation** (AirSim [68]): evaluations cover diverse outdoor scenarios, multiple altitudes and camera gimbal angles. UAV agents answer aerial VQA and execute VLN flight instructions (e.g., “hover directly over the pool in three to four meters altitude”).
- **Robotic Manipulation** (RLBench [33]): indoor workspaces with a curated object set (e.g., basket-

ball, blocks, drawer) and tasks spanning pick/place, open/close, and kinematic interactions, form the manipulation environment of Embodied4C. Object variations include size, shape, and material. Agents answer VQAs and perform VLN manipulation tasks (e.g., “close the bottom drawer of the cabinet”).

Due to space limitations, additional explanatory insights and examples are provided in Appendix 6.1 and Table 3.

### 3.4. Evaluation Protocol

Most existing benchmarks either rely on multiple-choice questions, which introduce inductive biases and allow models to exploit superficial answer patterns rather than demonstrate genuine reasoning [8, 102], or on traditional language metrics [4, 55], which have shown weak correlation with human judgment in multimodal and open-ended tasks [5, 46, 84]. To address these limitations, Embodied4C adopts an open-ended VQA format and uses a GPT-based scoring mechanism [77] for natural language answers, while dedicated quantitative metrics are applied to numerical responses. This design mitigates inductive answer biases and more faithfully captures semantic alignment between predictions and ground truth. Evaluation consists of two scoring processes, corresponding to VQA and VLN.

#### 3.4.1. VQA Scoring

The VQA evaluation measures how well agents produce correct, grounded answers to open-ended questions. Let  $Q = \{q_1, \dots, q_N\}$  denote the set of all questions, each with ground truth answer  $a_i$  and model prediction  $\hat{a}_i$ . We distinguish between free-form and numerical answers and apply complementary scoring schemes to balance linguistic fidelity and quantitative precision.

**Scoring.** For free-form answers, a VLM-judge assigns a continuous score in  $[0, 100]$ :

$$s(q_i) = \text{GPT}(\hat{a}_i, a_i). \quad (1)$$

For numerical answers, we apply a relative deviation formula that rewards proximity to the ground truth:

$$s(q_i) = \max \left( 0, 100 \cdot \left( 1 - \frac{|\hat{a}_i - a_i|}{0.01 \cdot |a_i|} \right) \right). \quad (2)$$

If  $\hat{a}_i$  is not numerical within a numerical question, GPT-based scoring is used as fallback enforcing numerical scoring through a structured prompt (cf. Table 6). In this implementation we use GPT-5 [54] as the VLM-judge.

**Aggregation.** We compute per-capability means over semantic, spatial, temporal, and physical subsets  $k$ :

$$S_{\text{VQA},k} = \frac{1}{|Q_k|} \sum_{q_i \in Q_k} s(q_i), \quad (3)$$

and average across capabilities to obtain the overall VQA score for each sub-benchmark:

$$S_{\text{VQA}} = \frac{1}{4} \sum_{k=1}^4 S_{\text{VQA},k}. \quad (4)$$

#### 3.4.2. VLN Scoring

In line with exam-style evaluation, each VLN task is probed only once, either with a binary pass/fail criterion for simple tasks or with a graded, distance-based score for more complex tasks. This design avoids repeated trials that could artificially inflate success rates, ensures comparability across agents under equal conditions, and reflects real-world scenarios where autonomous systems often have only a single opportunity to execute instructions correctly. Each VLN task consists of a natural language instruction  $I_j$  with a corresponding target condition (e.g., location, maneuver, etc.).

**Scoring.** For simple tasks, we apply a binary criterion:

$$s(I_j) = \begin{cases} 100, & \text{if } \theta_{\text{agt}} \in \Theta, \\ 0, & \text{otherwise,} \end{cases} \quad (5)$$

where  $\Theta$  denotes the set of task-dependent target conditions. A score of 100 points is awarded if the agent’s state  $\theta_{\text{agt}}$  satisfies all of the conditions in  $\Theta$ . For complex tasks, we use a graded scoring scheme that rewards partial, distance-based progress towards the target, with a maximum of 50 points unless all target conditions  $\Theta$  are fully satisfied. Let  $d_{\text{init}}$  be the initial distance to the target and  $d_{\text{agt}}$  the agent’s final distance to the target at the end of the VLN task episode. The VLN score is thus computed as:

$$s(I_j) = \begin{cases} 100, & \text{if } \theta_{\text{agt}} \in \Theta, \\ 50 \cdot \max \left( 0, \frac{d_{\text{init}} - d_{\text{agt}}}{d_{\text{init}}} \right), & \text{otherwise.} \end{cases} \quad (6)$$

This graded scoring formulation rewards partial progress while preserving strict success criteria, reflecting the realistic nature of single-attempt embodied evaluations. Further details on VLN scoring for each sub-benchmark are provided in Appendix 8.

**Aggregation.** The VLN score is averaged across all  $M$  tasks in each embodiment setup:

$$S_{\text{VLN}} = \frac{1}{M} \sum_{j=1}^M s(I_j). \quad (7)$$

### 3.5. Final Score Computation

For each sub-benchmark  $b \in \{1, 2, 3\}$  (driving, aerial, manipulation), the combined score is:

$$S_b = \frac{1}{2} (S_{\text{VQA}}^b + S_{\text{VLN}}^b), \quad (8)$$

while the overall benchmark score is the computed as the mean across embodiments:

$$S_{\text{total}} = \frac{1}{3} \sum_{b=1}^3 S_b. \quad (9)$$

These formulations equally weight VQA and VLN performance within each embodiment, while the aggregation across  $b$  ensures that all three embodiments contribute equally to the final score, which avoids biasing the benchmark toward a particular task type or embodiment. In addition, we report the mean score for generality (GEN) as a separate diagnostic axis to detect overfitting and assess robustness, avoiding score entanglement that could obscure capability-specific insights. The generality score is computed similar to Equation 1.

### 3.6. Diagnostics

In addition to aggregated scores, the benchmark records atomic logs for every VQA item and VLN trial. Each log entry contains: question/task id, scenario id, embodiment, sensor configuration, modality (RGB/grayscale), capability label (semantic/spatial/temporal/physical), ground truth, agent prediction, and the assigned numeric score. These records enable researchers to perform fine-grained capability-level error analysis, ablations, and cross-embodiment comparisons beyond aggregate scores.

## 4. Experiments

### 4.1. Experimental Setup

We evaluate a diverse set of models on the proposed Embodied4C benchmark, covering both pretrained foundation models (used with official weights and without task-specific finetuning) and state-of-the-art VLN models. The evaluated models include FastVLM-0.5B [38], Qwen2.5-VL-3B-Instruct [3], Gemma3-4B-IT [23], LLaMA 4 Maverick [52], Claude 3.7 Sonnet [2], Claude Sonnet 4.5 [1], GPT-4o [75], GPT-5-nano [54], GPT-5-mini [54], GPT-5 [54], Senna [34], OpenFly-Agent [22], OpenVLA [37], and MolmoAct [39]. The selection serves as the baseline for evaluating core value propositions of VLMs and also covers models with demonstrated capabilities in VQA and VLN across autonomous driving, aerial navigation, and robotic manipulation, while considering open-source availability. In Appendix 9, we provide a detailed comparison of state-of-the-art models in their respective domains, further motivating our selection of Senna, OpenFly-Agent, OpenVLA, and MolmoAct, based on their capabilities and relevance to our benchmark (cf. Tables 15–17).

### 4.2. Overall Benchmark Results

GPT-5-mini achieves the highest overall Embodied4C score (39.59), followed by GPT-5 (36.00). The Claude series

and LLaMA 4 Maverick cluster in the mid-range (28–31), while smaller models (Qwen2.5-VL and Gemma3-4B-IT) remain substantially weaker across embodiments. Domain-specialized vision-language-action (VLA) models such as Senna, OpenFly-Agent, OpenVLA, and MolmoAct exhibit near-zero performance in both VQA and VLN despite being optimized for action execution. Their performance profiles are further discussed in Appendix 10. An additional principal component analysis (PCA) decomposition in Appendix 10.2 reveals that these models form a distinct performance cluster characterized by limited linguistic grounding and narrow embodiment-specific priors.

### 4.3. Embodiment-wise Performance

**Autonomous Driving.** GPT-5-mini attains the highest score (40.11), with GPT-5 and GPT-4o following. Claude and Qwen/Gemma models show weaker spatial and temporal grounding, resulting in unstable VLN behavior. Domain-specialized driving VLAs do not transfer: Senna remains tied to its nuScenes training distribution and performs rather weak in CARLA scenario-level reasoning and control (cf. Appendix 8.1). **Aerial Navigation.** GPT-5-mini again leads (40.21), followed by GPT-5-nano and GPT-5. Performance generally degrades under large viewpoint shifts and dynamic 3D rotations. OpenFly-Agent, despite UAV training, collapses in Embodied4C due to strong overfitting to simulator-specific flight dynamics and state representations (cf. Appendix 8.2). **Robotic Manipulation.** GPT-5 (38.64) and GPT-5-mini (38.44) achieve the highest manipulation scores, driven by consistent semantic grounding and physical reasoning. Claude 4.5 is competitive but less spatially precise. OpenVLA fails entirely: language outputs degrade when the action head is bypassed, and action execution does not transfer to unseen object-environment configurations (cf. Appendix 8.3).

### 4.4. Modality-wise Performance (VQA vs. VLN)

VQA is consistently easier across all generalist models. OpenAI’s GPT-5 family [54] exhibits the smallest VQA-VLN gap, indicating stronger perception-action alignment. In contrast, VLA models collapse in VQA because their text-decoding pathways are under-optimized or unused during training. Moreover, when used in VLN mode, these models fail to transfer their action policies beyond their native training environments, showing strong embodiment overfitting and no cross-domain motor abstraction.

### 4.5. Capability-wise Analysis

Semantic and physical understanding contribute most to overall performance. Spatial and temporal reasoning remain the principal bottlenecks, leading to inconsistent action execution and lower VLN scores. Both, GPT-5 and GPT-5-mini, show balanced capability profiles with

Model	Autonomous Driving						Aerial Navigation					
	SEM	SPA	TEM	PHY	VLN	DS	SEM	SPA	TEM	PHY	VLN	AS
FastVLM-0.5B [38]	15.88	12.43	5.66	14.58	0.00	6.07	11.49	5.89	11.81	15.96	3.44	7.36
Qwen2.5-VL-3B-Instruct [3]	41.52	19.21	17.02	24.19	13.25	19.37	27.39	21.62	20.95	37.29	9.37	18.09
Gemma3-4B-IT [23]	34.22	17.78	21.91	25.70	15.56	20.23	33.39	21.26	18.61	28.39	5.54	15.48
LLaMA 4 Maverick [52]	58.86	35.31	27.94	53.64	<u>20.56</u>	32.25	45.55	19.15	25.96	34.85	23.52	27.45
Claude 3.7 Sonnet [2]	58.16	32.39	33.02	48.99	18.56	30.85	23.39	16.81	19.83	30.11	25.59	24.06
Claude Sonnet 4.5 [1]	63.51	31.01	39.90	50.64	18.94	32.60	36.82	24.47	34.06	41.10	27.54	30.82
GPT-4o [75]	<b>65.18</b>	<b>37.75</b>	<u>40.66</u>	46.91	19.62	33.62	38.83	24.38	35.32	34.85	24.55	28.95
GPT-5-nano [54]	40.38	25.49	32.54	41.21	16.69	25.80	<u>54.28</u>	<u>34.42</u>	34.51	47.71	26.66	34.70
GPT-5-mini [54]	60.23	<u>37.12</u>	38.66	<b>59.86</b>	<b>31.25</b>	<b>40.11</b>	<b>57.82</b>	<b>36.33</b>	<b>52.05</b>	<b>50.32</b>	<b>31.29</b>	<b>40.21</b>
GPT-5 [54]	64.50	35.97	<b>51.16</b>	<u>54.38</u>	16.75	<u>34.13</u>	50.92	34.36	<u>38.62</u>	<u>46.30</u>	27.92	<u>35.24</u>
Senna [34]	20.93	9.90	12.06	15.74	12.50	13.58	1.80	3.42	3.82	6.64	3.05	3.48
OpenFly-Agent [22]	0.00	0.00	0.00	0.00	12.44	6.22	0.00	0.00	0.00	0.00	3.24	1.62
OpenVLA [37]	0.00	0.00	0.00	0.00	0.00	0.00	0.00	0.00	0.00	0.00	1.85	0.92
MolmoAct [39]	0.04	0.02	0.00	0.03	2.88	1.45	0.00	0.04	0.02	0.00	3.73	1.87

(continued below)

Model	Robotic Manipulation						E4C-S ↑	Domain-far QA GEN
	SEM	SPA	TEM	PHY	VLN	MS		
FastVLM-0.5B [38]	18.30	15.28	13.06	17.69	0.00	8.04	7.16	25.39
Qwen2.5-VL-3B-Instruct [3]	48.05	35.32	30.99	48.22	0.62	20.63	19.36	91.37
Gemma3-4B-IT [23]	43.83	33.16	26.07	<u>51.38</u>	0.00	19.30	18.34	87.92
LLaMA 4 Maverick [52]	48.06	39.25	33.54	71.04	10.00	28.99	29.56	87.06
Claude 3.7 Sonnet [2]	54.21	42.51	43.62	72.51	5.00	29.11	28.01	98.02
Claude Sonnet 4.5 [1]	52.97	42.30	43.20	76.74	10.00	31.90	31.78	98.53
GPT-4o [75]	69.45	<u>47.40</u>	35.41	78.13	5.00	31.30	31.29	79.19
GPT-5-nano [54]	55.81	36.52	46.01	76.99	<u>12.07</u>	32.95	31.15	66.30
GPT-5-mini [54]	<b>72.89</b>	46.70	<b>52.29</b>	<b>86.18</b>	<b>12.36</b>	<u>38.44</u>	<b>39.59</b>	<b>99.97</b>
GPT-5 [54]	70.17	<b>55.66</b>	<u>52.04</u>	85.38	11.47	<b>38.64</b>	<u>36.00</u>	<u>99.13</u>
Senna [34]	10.70	13.31	12.01	27.38	0.00	7.92	8.33	59.08
OpenFly-Agent [22]	0.00	0.00	0.00	0.00	0.00	0.00	2.61	0.00
OpenVLA [37]	0.00	0.00	0.00	0.00	0.00	0.00	0.31	0.00
MolmoAct [39]	0.28	0.28	1.31	0.15	0.00	0.25	1.19	0.00

Table 2. **Capability-specific scores and overall Embodied4C score (E4C-S).** Models are evaluated across semantic (SEM), spatial (SPA), temporal (TEM), and physical understanding (PHY), as well as vision-language navigation (VLN). DS, AS, and MS denote driving, aerial, and manipulation scores of each sub-benchmark. **Generality (GEN) scores** are reported for domain-far questions, which are injected throughout standard scenario VQA tasks to assess model robustness and detect overfitting, computed analogously to Eq. 1 and independent of capability-specific performance. Higher is better (↑). **Bold** indicates the best score per column; underlined indicates the second best.

a low coefficient of variation ( $CV\%_{GPT-5} = 31.1\%$ ;  $CV\%_{GPT-5\text{-mini}} = 32.6\%$ ) through all capabilities and sub-benchmarks (cf. Figure 6). Domain-specialized VLA models exhibit flattened capability signatures near zero, indicating absence of genuine multimodal reasoning beyond policy regression. A detailed subcategory analysis in Appendix 10 reveals further insights (cf. Figure 5, 6).

#### 4.6. Generalization (GEN) Analysis

Most generalist models achieve high generalization scores, confirming robustness to irrelevant multimodal distractors. In contrast, VLA models and FastVLM degrade sharply, either hallucinating, over-attending to irrelevant input, or to synthetic control affordances learned during finetuning rather than the linguistic context. Qualitative examples can be observed in Figure 2.

#### 4.7. Discussion and Implications

The results highlight several structural trends in current multimodal and embodied models. **(i) Alignment over scale.** GPT-5-mini surpasses GPT-5 and other larger models, indicating that efficient cross-modal alignment and calibrated token interactions are more decisive than parameter count. Larger models without strengthened grounding exhibit high semantic capability but unstable spatial and temporal reasoning and therefore degrade in VLN. **(ii) Instruction tuning is indispensable.** Models lacking instruction tuning (e.g., FastVLM or domain-specific VLAs) fail to follow task structure and disregard VLN interface conventions. Effective embodied reasoning demands consistent linguistic grounding to map natural-language intent to executable actions and VQA. **(iii) Spatial and temporal reasoning remain limiting factors.** Even top-performing

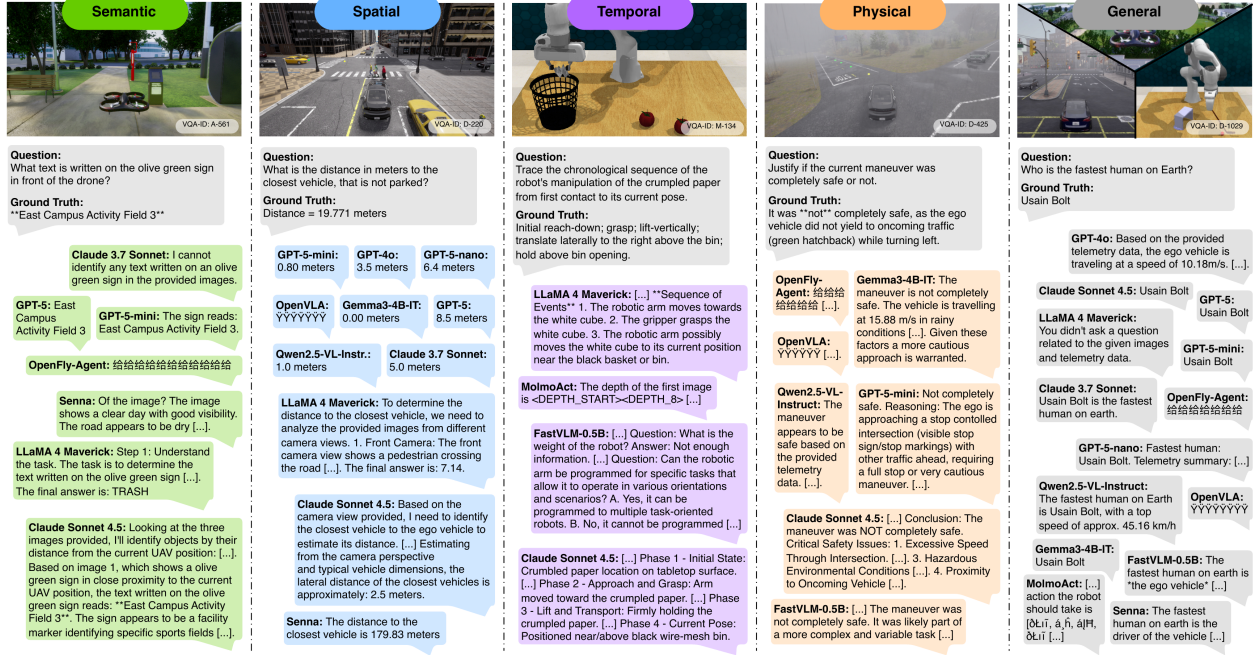


Figure 2. **Qualitative examples of Embodied4C VQA** across diverse benchmark scenarios and domains. The figure illustrates typical success and failure patterns for semantic, spatial, temporal, physical, and general reasoning across all tested models.

models struggle with persistent scene memory, viewpoint consistency, and long-horizon motion coherence. This suggests that current training pipelines do not sufficiently enforce geometric structure or temporal continuity, pointing to the need for inductive priors or explicit world modeling. **(iv) Domain-specialized VLA models do not generalize.** All tested VLAs perform near-zero outside their native training domains. When the action head is bypassed, language outputs collapse; when action execution is used, policies fail to transfer across embodiments and scenarios. These models optimize over narrow control priors rather than learning transferable scene understanding or reasoning (details in Appendix 9 and Appendix 10).

In summary, Embodied4C demonstrates that current foundation VLMs exhibit *generality* and *embodiment-awareness*: models such as GPT-5 maintain a relatively stable performance across embodiment changes and domain shifts but lack spatial and temporal reasoning capability. In contrast, domain-specialized VLAs fail to generalize beyond their native control priors, collapsing either in language output or action execution. Meanwhile, *interactivity* remains partially achieved: most VLMs can produce coherent, environment-aware answers, yet all models struggle to translate these into consistent long-horizon navigation, reflecting unresolved spatial and temporal grounding. Overall, generalizable embodied intelligence requires persistent world modeling and physically grounded representations, rather than additional scale or narrowly tuned action heads.

## 5. Conclusion

We presented **Embodied4C**, a closed-loop benchmark designed to evaluate core capabilities of VLMs in embodied reasoning and navigation across three heterogeneous embodiments: autonomous vehicles, UAVs, and robotic manipulators. Agents are assessed via both VQA and VLN, enabling fine-grained evaluation across four core understanding categories—semantic, spatial, temporal, and physical—each further divided into a total of 18 subcategories. This enables targeted model assessment and guidance for future research directions. By incorporating domain-far common-sense questions, Embodied4C explicitly probes generalization and overfitting, while comparisons across multiple embodiments highlight distinct strengths and weaknesses between pre-trained VLMs and task-specific expert models. Our results demonstrate that gaps in spatial and temporal reasoning directly manifest in degraded closed-loop execution, while domain-specialized agents remain tightly bound to their training distributions, underscoring the need for more general-purpose embodied reasoning and control agents that can generalize embodiments based on prompts.

**Future Work.** Future extensions include systematic evaluation of safety-critical behaviors, hallucination and failure modes, real-time model inference and latency. Furthermore, incorporating multi-agent scenarios and lifelong interaction tasks can extend the benchmark to comprehensively evaluate additional critical aspects of embodied agents.

## References

[1] AI Anthropic. Introducing claude sonnet 4.5, 2025. Available at: <https://www.anthropic.com>. 2, 6, 7, 8, 11

[2] AI Anthropic. The claude 3 model family: Opus, sonnet, haiku. Claude-3 Model Card, 2024. Available at: <https://www.anthropic.com>. 6, 7, 11

[3] Shuai Bai, Keqin Chen, Xuejing Liu, Jialin Wang, Wenbin Ge, Sibo Song, Kai Dang, Peng Wang, Shijie Wang, Jun Tang, Humen Zhong, Yuanzhi Zhu, Mingkun Yang, Zhao-hai Li, Jianqiang Wan, Pengfei Wang, Wei Ding, Zheren Fu, Yiheng Xu, Jiabo Ye, Xi Zhang, Tianbao Xie, Zesen Cheng, Hang Zhang, Zhibo Yang, Haiyang Xu, and Junyang Lin. Qwen2.5-vl technical report. *arXiv preprint arXiv:2502.13923*, 2025. 2, 6, 7, 10, 11

[4] Satanjeev Banerjee and Alon Lavie. Meteor: An automatic metric for mt evaluation with improved correlation with human judgments. In *Proceedings of the acl workshop on intrinsic and extrinsic evaluation measures for machine translation and/or summarization*, pages 65–72, 2005. 5, 2

[5] Kathrin Blagec, Georg Dorffner, Milad Moradi, Simon Ott, and Matthias Samwald. A global analysis of metrics used for measuring performance in natural language processing, 2022. 5

[6] Anthony Brohan, Noah Brown, Justice Carbajal, Yevgen Chebotar, Joseph Dabis, Chelsea Finn, Keerthana Gopalakrishnan, Karol Hausman, Alex Herzog, Jasmine Hsu, Julian Ibarz, Brian Ichter, Alex Irpan, Tomas Jackson, Sally Jesmonth, Nikhil J Joshi, Ryan Julian, Dmitry Kalashnikov, Yuheng Kuang, Isabel Leal, Kuang-Huei Lee, Sergey Levine, Yao Lu, Utsav Malla, Deeksha Manjunath, Igor Mordatch, Ofir Nachum, Carolina Parada, Jodilyn Peralta, Emily Perez, Karl Pertsch, Jornell Quiambao, Kanishka Rao, Michael Ryoo, Grecia Salazar, Pannag San keti, Kevin Sayed, Jaspair Singh, Sumedh Sontakke, Austin Stone, Clayton Tan, Huong Tran, Vincent Vanhoucke, Steve Vega, Quan Vuong, Fei Xia, Ted Xiao, Peng Xu, Sichun Xu, Tianhe Yu, and Brianna Zitkovich. Rt-1: Robotics transformer for real-world control at scale, 2023. 10

[7] Xu Cao, Tong Zhou, Yunsheng Ma, Wenqian Ye, Can Cui, Kun Tang, Zhipeng Cao, Kaizhao Liang, Ziran Wang, James M. Rehg, and Chao Zheng. Maplm: A real-world large-scale vision-language benchmark for map and traffic scene understanding. In *Proceedings of the IEEE/CVF Conference on Computer Vision and Pattern Recognition (CVPR)*, pages 21819–21830, 2024. 2, 3

[8] Nikhil Chandak, Shashwat Goel, Ameya Prabhu, Moritz Hardt, and Jonas Geiping. Answer matching outperforms multiple choice for language model evaluation, 2025. 2, 5

[9] Kai Chen, Yanze Li, Wenhua Zhang, Yanxin Liu, Pengxiang Li, Ruiyuan Gao, Lanqing Hong, Meng Tian, Xinhai Zhao, Zhenguo Li, Dit-Yan Yeung, Huchuan Lu, and Xu Jia. Automated evaluation of large vision-language models on self-driving corner cases, 2024. 2, 3

[10] Long Chen, Oleg Sinavski, Jan Hünermann, Alice Karnsund, Andrew James Willmott, Danny Birch, Daniel Maund, and Jamie Shotton. Driving with llms: Fusing object-level vector modality for explainable autonomous driving. In *2024 IEEE International Conference on Robotics and Automation (ICRA)*, pages 14093–14100, 2024. 8

[11] Yuan Chen, Zi-han Ding, Ziqin Wang, Yan Wang, Lijun Zhang, and Si Liu. Asynchronous large language model enhanced planner for autonomous driving. In *Computer Vision – ECCV 2024*, pages 22–38, Cham, 2025. Springer Nature Switzerland. 8

[12] An-Chieh Cheng, Hongxu Yin, Yang Fu, Qiushan Guo, Ruihan Yang, Jan Kautz, Xiaolong Wang, and Sifei Liu. Spatialrgpt: Grounded spatial reasoning in vision-language models. In *Advances in Neural Information Processing Systems*, pages 135062–135093. Curran Associates, Inc., 2024. 2, 3

[13] Zhili Cheng, Yuge Tu, Ran Li, Shiqi Dai, Jinyi Hu, Shengding Hu, Jiahao Li, Yang Shi, Tianyu Yu, Weize Chen, Lei Shi, and Maosong Sun. Embodiedeval: Evaluate multimodal llms as embodied agents, 2025. 3, 4

[14] Tushar Choudhary, Vikrant Dewangan, Shivam Chandhok, Shubham Priyadarshan, Anushka Jain, Arun K. Singh, Siddharth Srivastava, Krishna Murthy Jatavallabhula, and K. Madhava Krishna. Talk2bev: Language-enhanced bird’s-eye view maps for autonomous driving. In *2024 IEEE International Conference on Robotics and Automation (ICRA)*, pages 16345–16352, 2024. 2, 3

[15] Xinpeng Ding, Jianhua Han, Hang Xu, Xiaodan Liang, Wei Zhang, and Xiaomeng Li. Holistic autonomous driving understanding by bird’s-eye-view injected multi-modal large models. In *Proceedings of the IEEE/CVF Conference on Computer Vision and Pattern Recognition (CVPR)*, pages 13668–13677, 2024. 8

[16] Xinpeng Ding, Jianhua Han, Hang Xu, Xiaodan Liang, Wei Zhang, and Xiaomeng Li. Holistic autonomous driving understanding by bird’s-eye-view injected multi-modal large models. In *Proceedings of the IEEE/CVF Conference on Computer Vision and Pattern Recognition (CVPR)*, pages 13668–13677, 2024. 2, 3

[17] Yang Dong, Hansheng Liang, Mingliang Zhai, Cheng Li, Meng Xia, Xinglin Liu, Mengjingcheng Mo, Jiaxu Leng, Ji Tao, and Xinbo Gao. Bevlm: Got-based integration of bev and llm for driving with language. 2024. 8

[18] Alexey Dosovitskiy, German Ros, Felipe Codevilla, Antonio Lopez, and Vladlen Koltun. CARLA: An open urban driving simulator. In *Proceedings of the 1st Annual Conference on Robot Learning*, pages 1–16. PMLR, 2017. 4

[19] Yue Fan, Winson Chen, Tongzhou Jiang, Chun Zhou, Yi Zhang, and Xin Eric Wang. Aerial vision-and-dialog navigation, 2023. 3

[20] Haoyu Fu, Diankun Zhang, Zongchuang Zhao, Jianfeng Cui, Dingkang Liang, Chong Zhang, Dingyuan Zhang, Hongwei Xie, Bing Wang, and Xiang Bai. Orion: A holistic end-to-end autonomous driving framework by vision-language instructed action generation, 2025. 8

[21] Chen Gao, Baining Zhao, Weichen Zhang, Jinzhu Mao, Jun Zhang, Zhiheng Zheng, Fanhang Man, Jianjie Fang, Zile Zhou, Jinqiang Cui, Xinlei Chen, and Yong Li. Embod-

iedcity: A benchmark platform for embodied agent in real-world city environment, 2024. 3

[22] Yunpeng Gao, Chenhui Li, Zhongrui You, Junli Liu, Zhen Li, Pengan Chen, Qizhi Chen, Zhonghan Tang, Liansheng Wang, Penghui Yang, Yiwen Tang, Yuhang Tang, Shuai Liang, Songyi Zhu, Ziqin Xiong, Yifei Su, Xinyi Ye, Jianan Li, Yan Ding, Dong Wang, Zhigang Wang, Bin Zhao, and Xuelong Li. Openfly: A comprehensive platform for aerial vision-language navigation, 2025. 2, 3, 6, 7, 8, 11

[23] Gemma Team. Gemma 3 technical report, 2025. 2, 6, 7, 10, 11

[24] Ran Gong, Jiangyong Huang, Yizhou Zhao, Haoran Geng, Xiaofeng Gao, Qingyang Wu, Wensi Ai, Ziheng Zhou, Demetri Terzopoulos, Song-Chun Zhu, Baoxiong Jia, and Siyuan Huang. Arnold: A benchmark for language-grounded task learning with continuous states in realistic 3d scenes, 2023. 2, 3, 4

[25] Xianda Guo, Ruijun Zhang, Yiqun Duan, Yuhang He, Chenming Zhang, Shuai Liu, and Long Chen. Drivemllm: A benchmark for spatial understanding with multi-modal large language models in autonomous driving, 2024. 2, 3

[26] Wencheng Han, Dongqian Guo, Cheng-Zhong Xu, and Jianbing Shen. Dme-driver: Integrating human decision logic and 3d scene perception in autonomous driving, 2024. 8

[27] Wenlong Huang, Chen Wang, Ruohan Zhang, Yunzhu Li, Jiajun Wu, and Li Fei-Fei. Voxposer: Composable 3d value maps for robotic manipulation with language models, 2023. 10

[28] Zhijian Huang, Chengjian Feng, Feng Yan, Baihui Xiao, Zequn Jie, Yujie Zhong, Xiaodan Liang, and Lin Ma. Drivemm: All-in-one large multimodal model for autonomous driving, 2024. 8

[29] Zhijian Huang, Tao Tang, Shaoxiang Chen, Sihao Lin, Zequn Jie, Lin Ma, Guangrun Wang, and Xiaodan Liang. Making large language models better planners with reasoning-decision alignment. In *Computer Vision – ECCV 2024*, pages 73–90, Cham, 2025. Springer Nature Switzerland. 8

[30] Jyh-Jing Hwang, Runsheng Xu, Hubert Lin, Wei-Chih Hung, Jingwei Ji, Kristy Choi, Di Huang, Tong He, Paul Covington, Benjamin Sapp, Yin Zhou, James Guo, Dragomir Anguelov, and Mingxing Tan. Emma: End-to-end multimodal model for autonomous driving, 2024. 2, 8

[31] Yuichi Inoue, Yuki Yada, Kotaro Tanahashi, and Yu Yamaguchi. Nuscenes-mqa: Integrated evaluation of captions and qa for autonomous driving datasets using markup annotations. In *Proceedings of the IEEE/CVF Winter Conference on Applications of Computer Vision (WACV) Workshops*, pages 930–938, 2024. 2, 3

[32] Ahmed Jaafar, Shreyas Sundara Raman, Sudarshan Harithas, Yichen Wei, Sofia Juliani, Anneke Wernerfelt, Benedict Quartey, Ifrah Idrees, Jason Xinyu Liu, and Stefanie Tellex.  $\lambda$ : A benchmark for data-efficiency in long-horizon indoor mobile manipulation robotics, 2025. 3, 4

[33] Stephen James, Zicong Ma, David Rovick Arrojo, and Andrew J. Davison. Rlbench: The robot learning benchmark & learning environment, 2019. 3, 4, 5

[34] Bo Jiang, Shaoyu Chen, Bencheng Liao, Xingyu Zhang, Wei Yin, Qian Zhang, Chang Huang, Wenyu Liu, and Xinggang Wang. Senna: Bridging large vision-language models and end-to-end autonomous driving, 2024. 2, 6, 7, 8, 11

[35] Siwen Jiao, Yangyi Fang, Baoyun Peng, Wangqun Chen, and Bharadwaj Veeravalli. Lavida drive: Vision-text interaction vlm for autonomous driving with token selection, recovery and enhancement, 2025. 8

[36] Ye Jin, Ruoxuan Yang, Zhijie Yi, Xiaoxi Shen, Huiling Peng, Xiaoan Liu, Jingli Qin, Jiayang Li, Jintao Xie, Peizhong Gao, Guyue Zhou, and Jiangtao Gong. Surrealdriver: Designing llm-powered generative driver agent framework based on human drivers' driving-thinking data, 2024. 8

[37] Moo Jin Kim, Karl Pertsch, Siddharth Karamcheti, Ted Xiao, Ashwin Balakrishna, Suraj Nair, Rafael Rafailov, Ethan Foster, Grace Lam, Pannag Sanketi, Quan Vuong, Thomas Kollar, Benjamin Burchfiel, Russ Tedrake, Dorsa Sadigh, Sergey Levine, Percy Liang, and Chelsea Finn. Openvla: An open-source vision-language-action model, 2024. 2, 6, 7, 8, 10, 11

[38] Pavan Kumar, Anasosalu Vasu, Fartash Faghri, Chun-Liang Li, Cem Koc, Nate True, Albert Antony, Gokul Santhanam, James Gabriel, Peter Grasch, Oncel Tuzel, and Hadi Pouransari. Fastvlm: Efficient vision encoding for vision language models. In *Proceedings of the IEEE/CVF Conference on Computer Vision and Pattern Recognition (CVPR)*, 2025. 2, 6, 7, 11

[39] Jason Lee, Jiafei Duan, Haoquan Fang, Yuquan Deng, Shuo Liu, Boyang Li, Bohan Fang, Jieyu Zhang, Yi Ru Wang, Sangho Lee, Winson Han, Wilbert Pumacay, Angelica Wu, Rose Hendrix, Karen Farley, Eli VanderBilt, Ali Farhadi, Dieter Fox, and Ranjay Krishna. Molmoact: Action reasoning models that can reason in space, 2025. 2, 6, 7, 8, 10, 11

[40] Jungdae Lee, Taiki Miyanishi, Shuhei Kurita, Koya Sakamoto, Daichi Azuma, Yutaka Matsuo, and Nakamasa Inoue. Citynav: A large-scale dataset for real-world aerial navigation, 2025. 3

[41] Chengshu Li, Ruohan Zhang, Josiah Wong, Cem Gokmen, Sanjana Srivastava, Roberto Martín-Martín, Chen Wang, Gabrael Levine, Wensi Ai, Benjamin Martinez, Hang Yin, Michael Lingelbach, Minjune Hwang, Ayano Hiranaka, Sujay Garlanka, Arman Aydin, Sharon Lee, Jiankai Sun, Mona Anvari, Manasi Sharma, Dhruva Bansal, Samuel Hunter, Kyu-Young Kim, Alan Lou, Caleb R Matthews, Ivan Villa-Renteria, Jerry Huayang Tang, Claire Tang, Fei Xia, Yunzhu Li, Silvio Savarese, Hyowon Gweon, C. Karen Liu, Jiajun Wu, and Li Fei-Fei. Behavior-1k: A human-centered, embodied ai benchmark with 1,000 everyday activities and realistic simulation, 2024. 3, 4

[42] Jiahua Li, Zhiqi Li, and Tong Lu. Driving with internvl: Outstanding champion in the track on driving with language of the autonomous grand challenge at cvpr 2024, 2024. 8

[43] Xuanlin Li, Kyle Hsu, Jiayuan Gu, Karl Pertsch, Oier Mees, Homer Rich Walke, Chuyuan Fu, Ishikaa Lunawat, Isabel Sieh, Sean Kirmani, Sergey Levine, Jiajun Wu, Chelsea Finn, Hao Su, Quan Vuong, and Ted Xiao. Evaluating real-world robot manipulation policies in simulation, 2024. 3, 4

[44] Yue Li, Meng Tian, Zhenyu Lin, Jiangtong Zhu, Dechang Zhu, Haiqiang Liu, Zining Wang, Yueyi Zhang, Zhiwei Xiong, and Xinhai Zhao. Fine-grained evaluation of large vision-language models in autonomous driving, 2025. 3

[45] Shubo Liu, Hongsheng Zhang, Yuankai Qi, Peng Wang, Yuning Zhang, and Qi Wu. Aerialvln: Vision-and-language navigation for uavs, 2023. 2, 3, 8

[46] Yang Liu, Dan Iter, Yichong Xu, Shuohang Wang, Ruochen Xu, and Chenguang Zhu. G-eval: Nlg evaluation using gpt-4 with better human alignment, 2023. 5

[47] Artem Lykov, Valerii Serpiva, Muhammad Haris Khan, Oleg Sautenkov, Artyom Myshlyaev, Grik Tadevosyan, Yasheerah Yaqoot, and Dzmitry Tsetserukou. Cognitive-drone: A vla model and evaluation benchmark for real-time cognitive task solving and reasoning in uavs, 2025. 8

[48] Yingzi Ma, Yulong Cao, Jiachen Sun, Marco Pavone, and Chaowei Xiao. Dolphins: Multimodal language model for driving. In *Computer Vision – ECCV 2024*, pages 403–420, Cham, 2025. Springer Nature Switzerland. 8

[49] Jiageng Mao, Yuxi Qian, Junjie Ye, Hang Zhao, and Yue Wang. Gpt-driver: Learning to drive with gpt, 2023. 8

[50] Jiageng Mao, Junjie Ye, Yuxi Qian, Marco Pavone, and Yue Wang. A language agent for autonomous driving, 2024. 8

[51] Ana-Maria Marcu, Long Chen, Jan Hünermann, Alice Karnsund, Benoit Hanotte, Prajwal Chidananda, Saurabh Nair, Vijay Badrinarayanan, Alex Kendall, Jamie Shotton, Elahe Arani, and Oleg Sinavski. Lingoqa: Visual question answering for autonomous driving. In *Computer Vision – ECCV 2024*, pages 252–269, Cham, 2024. Springer Nature Switzerland. 2, 3

[52] AI Meta. The llama 4 herd: The beginning of a new era of natively multimodal ai innovation. Meta AI Blog, 2025. Retrieved April 09, 2025. 2, 6, 7, 8, 11

[53] Ming Nie, Renyuan Peng, Chunwei Wang, Xinyue Cai, Jianhua Han, Hang Xu, and Li Zhang. Reason2drive: Towards interpretable and chain-based reasoning for autonomous driving. In *Computer Vision – ECCV 2024*, pages 292–308, Cham, 2025. Springer Nature Switzerland. 2, 3, 8

[54] OpenAI. Introducing GPT-5. <https://openai.com/index/introducing-gpt-5/>, 2025. Accessed: 2025-04-05. 2, 5, 6, 7, 8, 11

[55] Kishore Papineni, Salim Roukos, Todd Ward, and Wei-Jing Zhu. Bleu: a method for automatic evaluation of machine translation. In *Proceedings of the 40th annual meeting of the Association for Computational Linguistics*, pages 311–318, 2002. 5, 2

[56] Carolina Parada. Gemini robotics: Bringing ai into the physical world. <https://deepmind.google/models/gemini-robotics/>, 2025. Accessed: 2025-08-12. 2

[57] SungYeon Park, MinJae Lee, JiHyuk Kang, Hahyeon Choi, Yoonah Park, Juhwan Cho, Adam Lee, and DongKyu Kim. Vlaad: Vision and language assistant for autonomous driving. In *Proceedings of the IEEE/CVF Winter Conference on Applications of Computer Vision (WACV) Workshops*, pages 980–987, 2024. 2, 3

[58] Taek-Hyun Park, Young-Jun Choi, Seung-Hoon Shin, Chang-Eun Lee, and Kwangil Lee. La-rcs: Llm-agent-based robot control system. *Sensors and Materials*, 37(7):3073, 2025. 8, 10

[59] Tianwen Qian, Jingjing Chen, Linhai Zhuo, Yang Jiao, and Yu-Gang Jiang. Nuscenes-qa: A multi-modal visual question answering benchmark for autonomous driving scenario. *Proceedings of the AAAI Conference on Artificial Intelligence*, 38(5):4542–4550, 2024. 2, 3

[60] Zhijie Qiao, Haowei Li, Zhong Cao, and Henry X. Liu. Lightemma: Lightweight end-to-end multimodal model for autonomous driving, 2025. 8

[61] Delin Qu, Haoming Song, Qizhi Chen, Yuanqi Yao, Xinyi Ye, Yan Ding, Zhigang Wang, JiaYuan Gu, Bin Zhao, Dong Wang, and Xuelong Li. Spatialvla: Exploring spatial representations for visual-language-action model, 2025. 10

[62] Katrin Renz, Long Chen, Ana-Maria Marcu, Jan Hünermann, Benoit Hanotte, Alice Karnsund, Jamie Shotton, Elahe Arani, and Oleg Sinavski. Carllava: Vision language models for camera-only closed-loop driving. *arXiv preprint arXiv:2406.10165*, 2024. 8

[63] Katrin Renz, Long Chen, Elahe Arani, and Oleg Sinavski. Simlingo: Vision-only closed-loop autonomous driving with language-action alignment, 2025. 8

[64] Enna Sachdeva, Nakul Agarwal, Suhas Chundi, Sean Roelofs, Jiachen Li, Mykel Kochenderfer, Chiho Choi, and Behzad Dariush. Rank2tell: A multimodal driving dataset for joint importance ranking and reasoning. In *Proceedings of the IEEE/CVF Winter Conference on Applications of Computer Vision (WACV)*, pages 7513–7522, 2024. 2, 3

[65] Oleg Sautenkov, Yasheerah Yaqoot, Artem Lykov, Muhammad Ahsan Mustafa, Grik Tadevosyan, Aibek Akhmetkazy, Miguel Altamirano Cabrera, Mikhail Martynov, Sausar Karaf, and Dzmitry Tsetserukou. Uav-vla: Vision-language-action system for large scale aerial mission generation. In *2025 20th ACM/IEEE International Conference on Human-Robot Interaction (HRI)*, pages 1588–1592, 2025. 8

[66] Pranav Saxena, Nishant Raghuvanshi, and Neena Goveas. Uav-vln: End-to-end vision language guided navigation for uavs, 2025. 8

[67] Hao Sha, Yao Mu, Yuxuan Jiang, Li Chen, Chenfeng Xu, Ping Luo, Shengbo Eben Li, Masayoshi Tomizuka, Wei Zhan, and Mingyu Ding. Languagempc: Large language models as decision makers for autonomous driving, 2023. 8

[68] Shital Shah, Debadeepa Dey, Chris Lovett, and Ashish Kapoor. Airsim: High-fidelity visual and physical simulation for autonomous vehicles, 2017. 4

[69] Hao Shao, Yuxuan Hu, Letian Wang, Guanglu Song, Steven L. Waslander, Yu Liu, and Hongsheng Li. Lm-drive: Closed-loop end-to-end driving with large language

models. In *Proceedings of the IEEE/CVF Conference on Computer Vision and Pattern Recognition (CVPR)*, pages 15120–15130, 2024. 8

[70] Mohit Shridhar, Lucas Manuelli, and Dieter Fox. Cliport: What and where pathways for robotic manipulation. In *Proceedings of the 5th Conference on Robot Learning*, pages 894–906. PMLR, 2022. 10

[71] Chonghao Sima, Katrin Renz, Kashyap Chitta, Li Chen, Hanxue Zhang, Chengan Xie, Jens Beißenwenger, Ping Luo, Andreas Geiger, and Hongyang Li. Drivelm: Driving with graph visual question answering. In *Computer Vision – ECCV 2024*, pages 256–274, Cham, 2025. Springer Nature Switzerland. 3, 4, 8

[72] Harsh Singh, Rocktim Jyoti Das, Mingfei Han, Preslav Nakov, and Ivan Laptev. Malmm: Multi-agent large language models for zero-shot robotics manipulation, 2025. 10

[73] Tin Stribor Sohn, Maximilian Dillitzer, Johannes Bach, Jason J. Corso, Tim Brühl, Robin Schwager, Tim Dieter Eberhardt, and Eric Sax. Drive4c: A closed-loop benchmark on what foundation models really need to be capable of for language-guided autonomous driving. In *Proceedings of the Computer Vision and Pattern Recognition Conference (CVPR) Workshops*, pages 3859–3869, 2025. 2, 3, 4

[74] Tin Stribor Sohn, Philipp Reis, Maximilian Dillitzer, Johannes Bach, Jason J. Corso, and Eric Sax. A framework for a capability-driven evaluation of scenario understanding for multimodal large language models in autonomous driving, 2025. 2, 3

[75] OpenAI Team. Gpt-4o system card, 2024. 2, 6, 7, 10, 11

[76] Kexin Tian, Jingrui Mao, Yunlong Zhang, Jiwan Jiang, Yang Zhou, and Zhengzhong Tu. Nuscenes-spatialqa: A spatial understanding and reasoning benchmark for vision-language models in autonomous driving, 2025. 2, 3

[77] Xiaoyu Tian, Junru Gu, Bailin Li, Yicheng Liu, Yang Wang, Zhiyong Zhao, Kun Zhan, Peng Jia, Xianpeng Lang, and Hang Zhao. Drivevilm: The convergence of autonomous driving and large vision-language models, 2024. 5, 7, 8

[78] Dian Wang, Colin Kohler, Xupeng Zhu, Mingxi Jia, and Robert Platt. Bulletarm: An open-source robotic manipulation benchmark and learning framework, 2022. 3, 4

[79] Junming Wang, Xingyu Zhang, Zebin Xing, Songen Gu, Xiaoyang Guo, Yang Hu, Ziyi Song, Qian Zhang, Xiaoxiao Long, and Wei Yin. He-drive: Human-like end-to-end driving with vision language models, 2024. 8

[80] Shihao Wang, Zhiding Yu, Xiaohui Jiang, Shiyi Lan, Min Shi, Nadine Chang, Jan Kautz, Ying Li, and Jose M. Alvarez. Omnidrive: A holistic llm-agent framework for autonomous driving with 3d perception, reasoning and planning, 2024. 8

[81] Wenhui Wang, Jiangwei Xie, ChuanYang Hu, Haoming Zou, Jianan Fan, Wenwen Tong, Yang Wen, Silei Wu, Hanming Deng, Zhiqi Li, Hao Tian, Lewei Lu, Xizhou Zhu, Xiaogang Wang, Yu Qiao, and Jifeng Dai. Drivemlm: Aligning multi-modal large language models with behavioral planning states for autonomous driving, 2023. 8

[82] Xiangyu Wang, Donglin Yang, Ziqin Wang, Hohin Kwan, Jinyu Chen, Wenjun Wu, Hongsheng Li, Yue Liao, and Si Liu. Towards realistic uav vision-language navigation: Platform, benchmark, and methodology, 2024. 3, 4

[83] Julong Wei, Shanshuai Yuan, Pengfei Li, Qingda Hu, Zhongxue Gan, and Wenchao Ding. Occllama: An occupancy-language-action generative world model for autonomous driving, 2024. 8

[84] Genta Indra Winata, David Anugraha, Lucky Susanto, Garry Kuwanto, and Derry Tanti Wijaya. Metametrics: Calibrating metrics for generation tasks using human preferences, 2025. 5

[85] Lik Hang Kenny Wong, Xueyang Kang, Kaixin Bai, and Jianwei Zhang. A survey of robotic navigation and manipulation with physics simulators in the era of embodied ai, 2025. 2

[86] Dongming Wu, Wencheng Han, Tiancai Wang, Yingfei Liu, Xiangyu Zhang, and Jianbing Shen. Language prompt for autonomous driving, 2023. 2, 3

[87] Jianqiang Xiao, Yuexuan Sun, Yixin Shao, Boxi Gan, Rongqiang Liu, Yanjing Wu, Weili Guan, and Xiang Deng. Uav-on: A benchmark for open-world object goal navigation with aerial agents, 2025. 3, 4

[88] Shaoyuan Xie, Lingdong Kong, Yuhao Dong, Chonghao Sima, Wenwei Zhang, Qi Alfred Chen, Ziwei Liu, and Liang Pan. Are vlms ready for autonomous driving? an empirical study from the reliability, data, and metric perspectives, 2025. 2, 3

[89] Shuo Xing, Chengyuan Qian, Yuping Wang, Hongyuan Hua, Kexin Tian, Yang Zhou, and Zhengzhong Tu. Open-emma: Open-source multimodal model for end-to-end autonomous driving, 2025. 8

[90] Yi Xu, Yuxin Hu, Zaiwei Zhang, Gregory P. Meyer, Siva Karthik Mustikovela, Siddhartha Srinivasa, Eric M. Wolff, and Xin Huang. Vlm-ad: End-to-end autonomous driving through vision-language model supervision, 2024. 8

[91] Zhenhua Xu, Yujia Zhang, Enze Xie, Zhen Zhao, Yong Guo, Kwan-Yee K. Wong, Zhenguo Li, and Hengshuang Zhao. Drivegpt4: Interpretable end-to-end autonomous driving via large language model. *IEEE Robotics and Automation Letters*, 9(10):8186–8193, 2024. 8

[92] Rui Yang, Hanyang Chen, Junyu Zhang, Mark Zhao, Cheng Qian, Kangrui Wang, Qineng Wang, Teja Venkat Koripella, Marziyeh Movahedi, Manling Li, Heng Ji, Huan Zhang, and Tong Zhang. Embodiedbench: Comprehensive benchmarking multi-modal large language models for vision-driven embodied agents, 2025. 3, 4

[93] Senqiao Yang, Jiaming Liu, Ray Zhang, Mingjie Pan, Zoey Guo, Xiaocqi Li, Zehui Chen, Peng Gao, Yandong Guo, and Shanghang Zhang. Lidar-llm: Exploring the potential of large language models for 3d lidar understanding, 2023. 8

[94] Fanglong Yao, Yuanchang Yue, Youzhi Liu, Xian Sun, and Kun Fu. Aeroverse: Uav-agent benchmark suite for simulating, pre-training, finetuning, and evaluating aerospace embodied world models, 2024. 3

[95] Hui Ye, Rajshekhar Sunderraman, and Shihao Ji. Uav3d: A large-scale 3d perception benchmark for unmanned aerial vehicles, 2024. 3

[96] Jianhao Yuan, Shuyang Sun, Daniel Omeiza, Bo Zhao, Paul Newman, Lars Kunze, and Matthew Gadd. Rag-driver: Generalisable driving explanations with retrieval-augmented in-context learning in multi-modal large language model, 2024. 8

[97] Tong Zeng, Longfeng Wu, Liang Shi, Dawei Zhou, and Feng Guo. Are vision llms road-ready? a comprehensive benchmark for safety-critical driving video understanding, 2025. 3

[98] Tianyuan Zhang, Ting Jin, Lu Wang, Jiangfan Liu, Siyuan Liang, Mingchuan Zhang, Aishan Liu, and Xianglong Liu. Bench2advlm: A closed-loop benchmark for vision-language models in autonomous driving, 2025. 2, 3

[99] Xinyuan Zhang, Yonglin Tian, Fei Lin, Yue Liu, Jing Ma, Kornélia Sára Szatmáry, and Fei-Yue Wang. Logisticsvln: Vision-language navigation for low-altitude terminal delivery based on agentic uavs, 2025. 8

[100] Yuhang Zhang, Haosheng Yu, Jiaoping Xiao, and Mir Feroskhan. Grounded vision-language navigation for uavs with open-vocabulary goal understanding, 2025. 8

[101] Enyu Zhao, Vedant Raval, Hejia Zhang, Jiageng Mao, Zeyu Shangguan, Stefanos Nikolaidis, Yue Wang, and Daniel Seita. Manipbench: Benchmarking vision-language models for low-level robot manipulation, 2025. 3, 4

[102] Chujie Zheng, Hao Zhou, Fandong Meng, Jie Zhou, and Minlie Huang. Large language models are not robust multiple choice selectors, 2024. 2, 5

[103] Kaizhi Zheng, Xiaotong Chen, Odest Chadwicke Jenkins, and Xin Wang. Vlmbench: A compositional benchmark for vision-and-language manipulation. In *Advances in Neural Information Processing Systems*, pages 665–678. Curran Associates, Inc., 2022. 3, 4

[104] Xingcheng Zhou, Xuyuan Han, Feng Yang, Yunpu Ma, and Alois C. Knoll. Opendrivevla: Towards end-to-end autonomous driving with large vision language action model, 2025. 7, 8

[105] Yunsong Zhou, Linyan Huang, Qingwen Bu, Jia Zeng, Tianyu Li, Hang Qiu, Hongzi Zhu, Minyi Guo, Yu Qiao, and Hongyang Li. Embodied understanding of driving scenarios. In *Computer Vision – ECCV 2024*, pages 129–148, Cham, 2025. Springer Nature Switzerland. 8

[106] Brianna Zitkovich, Tianhe Yu, Sichun Xu, Peng Xu, Ted Xiao, Fei Xia, Jialin Wu, Paul Wohlhart, Stefan Welker, Ayzaan Wahid, Quan Vuong, Vincent Vanhoucke, Huong Tran, Radu Soricut, Anikait Singh, Jaspiar Singh, Pierre Sermanet, Pannag R. Sanketi, Grecia Salazar, Michael S. Ryoo, Krista Reymann, Kanishka Rao, Karl Pertsch, Igor Mordatch, Henryk Michalewski, Yao Lu, Sergey Levine, Lisa Lee, Tsang-Wei Edward Lee, Isabel Leal, Yuheng Kuang, Dmitry Kalashnikov, Ryan Julian, Nikhil J. Joshi, Alex Irpan, Brian Ichter, Jasmine Hsu, Alexander Herzog, Karol Hausman, Keerthana Gopalakrishnan, Chuyuan Fu, Pete Florence, Chelsea Finn, Kumar Avinava Dubey, Danny Driess, Tianli Ding, Krzysztof Marcin Choromanski, Xi Chen, Yevgen Chebotar, Justice Carbalal, Noah Brown, Anthony Brohan, Montserrat Gonzalez Arenas, and Kehang Han. Rt-2: Vision-language-action models transfer web knowledge to robotic control. In *Proceedings of The 7th Conference on Robot Learning*, pages 2165–2183. PMLR, 2023. 8, 10

# Embodied4C: Measuring What Matters for Embodied Vision-Language Navigation

## Supplementary Material

### 6. Benchmark Statistics and Settings

#### 6.1. VQA and VLN Distributions

The distribution of questions across the three sub-benchmarks and the main Embodied4C benchmark is detailed in Figure 3. Each benchmark consists of two types of natural language queries: VQA questions and VLN instructions. VQA is split in four main- and 18 subcategories:

- **SEM** (semantic): Questions related to object properties. Sub-categories include CL (classes), AT (attributes), and ST (states).
- **SPA** (spatial): Questions focusing on an object’s location and relationships to its surroundings. Sub-categories are LC (location), DT (distance), OR (orientation), TP (topology), CT (counting), R/S (relative size), R/P (relative position), and R/D (relative distance).
- **TEM** (temporal): Questions that require understanding of events over time. Sub-categories include MT (movement and time), S/M (short-term memory), and L/M (long-term memory).
- **PHY** (physical): Questions that test knowledge of physical understanding and situational laws. Sub-categories are MD (model dynamics), CS (constraints), M/P (material properties), and E/E (environmental effects).

The VQA questions are balanced across the four main reasoning categories—semantic, spatial, temporal, and physical—while additional domain-far questions test generalization beyond perceived scenarios. Specifically, autonomous driving includes 383 VQA pairs (59 semantic, 123 spatial, 58 temporal, 89 physical) plus 54 domain-far questions, aerial navigation comprises 358 VQA pairs (71 semantic, 143 spatial, 54 temporal, 49 physical) with 41 domain-far questions, and robotic manipulation contains 408 VQA pairs (67 semantic, 165 spatial, 68 temporal, 78 physical) along with 30 domain-far questions (cf. Figure 3). For VLN, tasks span a spectrum of difficulty to probe both basic and advanced embodied reasoning. Easy tasks verify understanding of the action space, such as engaging the handbrake and low-beam lights simultaneously or correctly closing the gripper, and are evaluated with a pass/fail criterion. Harder tasks test multi-step, real-world reasoning, e.g., navigating a busy intersection, landing in the middle circle of a football field, or shooting a basketball into a hoop. Autonomous driving thereby provides 16 VLN tasks, aerial navigation 22 tasks, and robotic manipulation 20 tasks (cf. Figure 3). For more details about VLN tasks, see Section 8 in the Appendix. The full Embod-

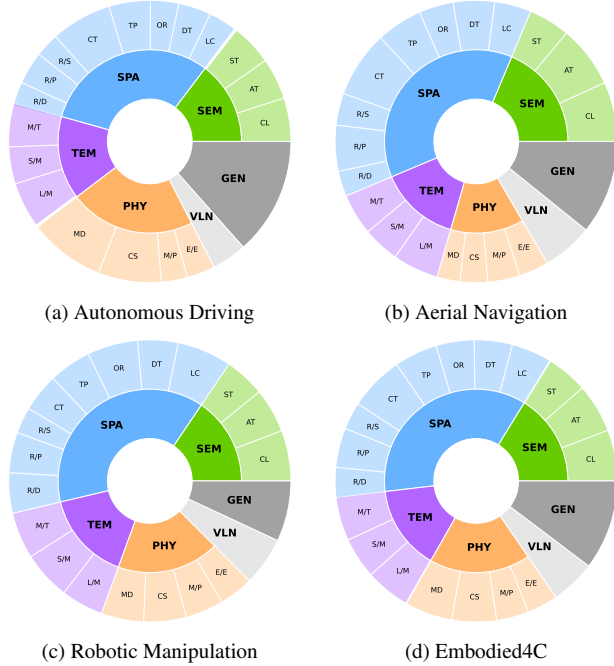


Figure 3. **Distributions for VQA questions and VLN instructions** across all three sub-benchmarks and Embodied4C.

ied4C benchmark is a combination of these, totaling 1.149 VQA questions and 58 VLN task instructions of varying difficulty. Table 3 provides examples of each category and sub-benchmark.

#### 6.2. Autonomous Agent System Prompts

To ensure consistent, reproducible, and semantically grounded evaluation of our VLM agents across diverse embodied tasks, we define three core system prompts that govern the behavior of both the *agent under test* and the *evaluation judge*. These prompts are engineered to enforce precision, domain adaptation, and scoring fidelity—critical for benchmarking open-ended, embodied reasoning in real-world simulation environments.

One system prompt (cf. Table 4) configures the **VLM-agent under test**, instructing it to operate as a general-purpose embodied reasoner across three distinct domains: autonomous driving, aerial navigation, and robotic manipulation. The prompt enforces strict adherence to sensor inputs, task instructions, and modality-aware reasoning—preventing hallucination and anchoring responses in observ-

Sub-Benchmark	Task	Category	Example
Autonomous Driving	VQA	SEM	“What is the type of lane the ego vehicle is currently situated on?”
	VQA	SPA	“Give back the distance in meters to the closest vehicle.”
	VQA	TEM	“How many vehicles have been passed throughout the whole scenario?”
	VQA	PHY	“Describe the vehicles current dynamic state of driving.”
	VLN	–	“Follow the leading vehicle within a follow distance of 5-20m for at least 100m.”
Aerial Navigation	VQA	SEM	“What color are the trash bins in the park?”
	VQA	SPA	“How many swings are present on the boat-swing structure?”
	VQA	TEM	“Tell the sequence of actions lastly performed by the ego agent drone.”
	VQA	PHY	“What needs to be considered when trying to land on the beach volleyball field?”
	VLN	–	“From your current position, fly towards the Merry-go-round and land on its inner platform.”
Robotic Manipulation	VQA	SEM	“What is the state of the middle drawer in the cabinet?”
	VQA	SPA	“Rank all three balls by their horizontal distance from the robot’s gripper, closest first.”
	VQA	TEM	“Which main object showed noticeable movement over the last frames?”
	VQA	PHY	“What type of kinematic model best describes the robot arm in this scene?”
	VLN	–	“Move the robot arm to pick up the rubbish and put it into the bin.”
All	VQA	GEN	“What is the term for a score of one under par in golf?”
	VQA	GEN	“Why do birds not get shocked when sitting on high-voltage power lines?”

Table 3. **Example VQA questions and VLN instructions** across sub-benchmarks and reasoning categories.

Systemprompt of the VLM-Agent Under Test	
You are an embodied multimodal reasoning agent capable of operating autonomous systems and answer questions grounded in your surrounding. Your task is to interpret multimodal inputs (images, video, point clouds, sensor data, text) from varying sensor setups and provide correct and concise control commands/actions or answers.	
You are able to operate in multiple embodiment domains: autonomous driving, aerial drone navigation, and manipulation in general robotics. You may receive different sensor sets depending on the embodiment context. Always adapt your reasoning to the available modalities.	
<b>Your objectives:</b>	
<ol style="list-style-type: none"> <li>1. Respond to general questions using concise and common knowledge-based reasoning.</li> <li>2. Answer questions about the environment and scenarios accurately based on the available sensor data.</li> <li>3. Follow instructions for controlling the embodiment (driving, flying, grasping, moving, etc.) exactly as stated in the query.</li> <li>4. Justify decisions with situational reasoning when required.</li> <li>5. Be concise, precise, and unambiguous in your responses on questions and instructions.</li> <li>6. <b>IMPORTANT:</b> Always adhere strictly to the task or instruction given in the prompt. Never assume missing information, only reason based on given input.</li> </ol>	

Table 4. **System prompt for the VLM-agent under test.** This prompt specifies the operational role of the model being evaluated. The agent must interpret multimodal sensor inputs across three embodiment domains (driving, UAV navigation, and robotic manipulation) to answer questions and execute control instructions. The design enforces concise, precise, and task-grounded reasoning without assumptions beyond the provided input.

able reality. For each domain, we additionally extend the system prompt with domain-specific interface instructions that expose only the permissible action space for the respective platform and explicitly define the required output format for downstream control execution in VLN tasks.

Two additional system prompts define the operational logic of our **VLM-judge** GPT-5 [54], which scores agent responses either (1) semantically against open-ended ground truth references (cf. Table 5), or (2) numerically using a deterministic function for quantitative outputs (cf. Table 6). This dual scoring mechanism ensures robust evaluation across both qualitative reasoning and metric-sensitive tasks, circumventing the limitations of discrete-choice formats and the misalignment of lexical overlap metrics such as BLEU [55] and METEOR [4] with human judgment.

Together, these prompts form the backbone of our evaluation protocol, enabling scalable, automated, and semantically consistent assessment of embodied agent performance in complex, open-world scenarios.

## 7. Multi-Embodiment Sensor Setups

### 7.1. Driving Agent Setups

To ensure realism and diversity, we adopt sensor configurations that mirror real-world automotive deployments. All sensors are mounted on a single ego vehicle (Lincoln MKZ 2020) at physically plausible, industry-inspired locations. For clarity and readability, the exact positions are omitted from Table 10; they correspond to the extents of the vehicle category and vary in  $x$ ,  $y$ , and  $z$ , depending on the vehicle

#### Systemprompt of the VLM-judge for GPT-Scoring

You are a precise evaluator of open-ended answers based on a ground truth reference. Your goal is to assign a continuous score between 0.0 and 100.0 that reflects how well the given answer semantically and contextually matches the intended reference.

##### Instructions:

- **Evaluate Meaning, Correctness, and Completeness:** Focus on whether the answer accurately conveys the intended meaning, is factually correct, and covers all necessary details as reflected in the reference answer.
- **Perfect Score (100.0):** Award a perfect score only if the answer fully captures the reference meaning and is entirely consistent with the ground truth. Paraphrasing and different wording are acceptable, provided the content is factually correct and complete.
- **Use Continuous Scoring:** Assign scores on a continuous scale (e.g., 91.5, 74.1, 23.7, etc.), avoiding coarse intervals like 50.0 or 80.0. This ensures nuanced scoring that reflects subtle differences in quality.
- **Minor Wordings Differences:** Do not penalize for minor differences in phrasing if the information is complete and correct.
- **Be Strict with Misinformation:** Apply strict penalties if the answer contains incorrect information, is incomplete, or contradicts the ground truth. For example, errors in directionality (e.g., left/right confusion), numerical inaccuracies, errors in output formatting, or logical inconsistencies should result in noticeable deductions.
- **Consistency in Judgment:** Apply these criteria consistently across all answers to maintain a fair and objective evaluation.

##### Scoring Scale:

- **100.0:** Meaningfully and fully aligned with the reference (even with paraphrasing or expansion).
- **80.0–99.0:** Mostly correct, only minor omissions or minor ambiguity.
- **50.0–79.0:** Partial understanding; some relevant info but lacks completeness or clarity.
- **10.0–49.0:** Low relevance; core idea is missing or answer is mostly off-target.
- **0.0:** Completely wrong or irrelevant.

Respond only with a single float value (e.g. 63.8). Do not include any explanation.

**Table 5. System prompt for the VLM-judge.** This prompt defines the evaluation protocol for GPT-based scoring of free-form answers. The judge assigns continuous scores between 0.0 and 100.0, reflecting semantic and contextual alignment with the ground-truth reference, while penalizing misinformation, incompleteness, and logical inconsistencies.

#### Systemprompt of the VLM-judge for numerical scoring

You are a precise evaluator of answers against a provided numeric ground truth reference. Your task is to assign a continuous score between 0.0 and 100.0 according to the numeric scoring function below. If the answer is given as text, you must extract the relevant numeric value before applying the function.

##### Scoring Function (normalized, then scaled to 0–100):

```
def numeric_score(llm_answer, groundtruth):
    try:
        llm_answer = abs(float(llm_answer))
    except:
        return 0.0

    if groundtruth == 0:
        if llm_answer == 0.0:
            return 100.0
        else:
            return 0.0

    if 0.9 * groundtruth <= llm_answer <= 1.1 * groundtruth:
        return 100.0 * (1 - abs(llm_answer - groundtruth) / (0.1 * groundtruth))
    else:
        return 0.0
```

##### Scoring Instructions:

- Extract the numeric prediction from the answer if it is embedded in text.
- Apply the above numeric\_score function to (llm\_answer, groundtruth).
- If no numeric value can be extracted, assign 0.0.
- Do not apply semantic/qualitative criteria; this evaluation is purely numeric.

##### Output Format:

Respond only with a single float value (e.g., 87.4). Do not include explanations.

**Table 6. System prompt for numerical scoring by the VLM-judge.** This prompt defines the formula to be applied as fallback GPT-based scoring of numerical-only answers. The judge assigns continuous scores between 0.0 and 100.0, replicating the numerical scoring functionality to full-text answers.

for which each sensor stack was originally designed. Each scenario is assigned a dedicated sensor stack that is loaded at the beginning of the episode, preserving physical plausi-

bility while simplifying runtime management.

This design enables two complementary evaluations of generalization: (i) embodiment generalization within a sin-

Action space prompt for ground vehicle driving in CARLA

**Specific System Instruction:**

You control the ego vehicle in a CARLA autonomous driving simulation. Your **sole output** must be a **single JSON object** representing the vehicles control action at each step. The JSON structure must **exactly** follow the format below and must not contain any explanations, text, or extra keys:

```
```json
{
  "throttle": 0.0,
  "brake": 0.0,
  "steer": 0.0,
  "hand_brake": false,
  "reverse": false,
  "gear": 1,
  "manual_gear_shift": false,
  "lights": {
    "position": false,
    "low_beam": false,
    "fog": false,
    "high_beam": false,
    "left_blinker": false,
    "right_blinker": false,
    "interior": false
  }
}
```

```

All values must be set to appropriate floats, booleans, or integers.

- 'throttle' and 'brake' are floats  $\in [0.0, 1.0]$ .
- 'steer' is a float  $\in [-1.0, 1.0]$ .
- 'hand\_brake', 'reverse', and all 'lights' fields are booleans.
- 'gear' is an integer.
- 'manual\_gear\_shift' is boolean.

You **must not** output natural language, reasoning steps, or additional formatting. You **must only return this JSON object** per step with the **specific control values required to complete the scenario**.

**Table 7. Action space prompt for driving tasks.** This prompt specifies the action space and interface of our driving simulator for the VLM under test. Additional parsing is applied to enforce the expected structure where feasible.

gle vehicle platform equipped with heterogeneous sensor layouts, and (ii) sensor-agnostic reasoning, i.e., assessing whether a single model can operate robustly across distinct sensor configurations without retraining or architectural modification. By varying the complete sensor suite between scenarios, the setup enforces robustness to realistic sensor heterogeneity while ensuring deterministic and reproducible experimental conditions.

## 7.2. UAV Agent Setups

Following the standard multirotor configuration provided by AirSim [68], all UAV scenarios are executed using a quadcopter platform equipped with a predefined sensor suite. Each scenario variant employs a distinct sensor configuration (cf. Table 11), comprising at minimum one RGB and one depth camera to ensure sufficient perceptual grounding for VQA and navigation tasks. In addition, comprehensive telemetry data are continuously streamed to the agent, including 3D pose ( $x, y, z$ ), orientation (roll, pitch, yaw), linear speed, and altitude above sea level. These mea-

Action space prompt for UAV navigation on Microsoft AirSim

**Specific System Instruction:**

You control the ego drone in a Microsoft AirSim drone navigation simulation. Your **sole output** must be a **single JSON object** representing the drones control action at each step. The JSON structure must **exactly** follow the format below and must not contain any explanations, text, or extra keys:

```
```json
{
  "vx": 0.0,
  "vy": 0.0,
  "vz": 0.0,
  "duration": 1.0,
  "yaw_rate": 0.0
}
```

```

All values must be set to appropriate floats.

- 'vx': forward/backward velocity in m/s (positive = forward)
- 'vy': right/left velocity in m/s (positive = right)
- 'vz': vertical velocity in m/s (positive = DOWN, negative = UP)
- 'duration': how long to apply this command, in seconds (e.g., 1.0)
- 'yaw\_rate': rotation speed in degrees per second (positive = turn right, negative = turn left)

You **must not** output natural language, reasoning steps, or additional formatting. You **must only return this JSON object** per step with the **specific control values required to complete the scenario**.

**Table 8. Action space prompt for UAV navigation tasks.** This prompt specifies the action space and interface of our drone simulator for the VLM under test. Additional parsing is applied to enforce the expected structure where feasible.

Action space prompt for robotic manipulation on RLBench

**Specific System Instruction:**

You control the robot arm in the RLbench simulation. Your **sole output** must be a **single array** representing the manipulators control action at each step. The array structure must **exactly** follow the format below and must not contain any explanations or text:

```
[0.0, 0.0, 0.0, 0.0, 0.0, 0.0, 0.0, 0.0]
```

All values must be set to appropriate floats.

- 'joint\_positions' (first seven entries): list of 7 floats representing the robot arm joint positions
- 'gripper' (last entry): float representing the gripper state (1.0 = fully open, 0.0 = fully closed)

You **must not** output natural language, reasoning steps, or additional formatting. You **must only return this array** per step with the **specific control values required to complete the scenario**.

**Table 9. Action space prompt for manipulation tasks.** This prompt specifies the action space and interface of our robotic simulator for the VLM under test. Additional parsing is applied to enforce the expected structure where feasible.

surements enable accurate state estimation and closed-loop control supervision.

To evaluate robustness and environmental generalization, experiments are conducted across five distinct outdoor environments in AirSim, each subjected to varying weather conditions such as illumination shifts, wind, and precipitation. This multi-environment design enforces cross-

| Vehicle        | Sensor Type    | Count | Position(s)          | Resolution / Specs           |
|----------------|----------------|-------|----------------------|------------------------------|
| Sportscar      | RGB Camera     | 6     | F, B, FR, FL, BR, BL | 1280×720 px, FOV 100°        |
|                | MRR            | 4     | FR, FL, BR, BL       | Range 70 m, FOV 90°H / 20°V  |
|                | LRR            | 1     | F                    | Range 250 m, FOV 20°H / 14°V |
|                | GNSS + IMU     | 1+1   | Center               | 20 Hz                        |
| Mid-Size Sedan | Speedometer    | 1     | —                    | 20 Hz                        |
|                | RGB Camera     | 4     | F, B, R, L           | 1280×720 px, FOV 100°        |
|                | Fisheye Camera | 2     | R, L                 | 1088×576 px, FOV 160°        |
|                | GNSS + IMU     | 1+1   | Center               | 20 Hz                        |
| Station Wagon  | Speedometer    | 1     | —                    | 20 Hz                        |
|                | Fisheye Camera | 4     | F, B, R, L           | 1088×576 px, FOV 160°        |
|                | LRR            | 1     | F                    | Range 250 m, FOV 20°H / 14°V |
|                | GNSS + IMU     | 1+1   | Center               | 20 Hz                        |
| SUV            | Speedometer    | 1     | —                    | 20 Hz                        |
|                | HD Map         | 1     | —                    | OpenDRIVE, static            |
|                | RGB Camera     | 6     | F, B, FR, FL, BR, BL | 1280×720 px, FOV 100°        |
|                | LiDAR          | 1     | Roof center          | 32 ch, 80 m, 360°H, ±30°V    |
| Van            | GNSS + IMU     | 1+1   | Center               | 20 Hz                        |
|                | Speedometer    | 1     | —                    | 20 Hz                        |
|                | HD Map         | 1     | —                    | OpenDRIVE, static            |
|                | RGB Camera     | 6     | F, B, FR, FL, BR, BL | 1280×720 px, FOV 100°        |
| Van            | LiDAR          | 1     | Roof center          | 32 ch, 80 m, 360°H, ±30°V    |
|                | MRR            | 4     | FR, FL, BR, BL       | Range 70 m, FOV 90°H / 20°V  |
|                | GNSS + IMU     | 1+1   | Center               | 20 Hz                        |
|                | Speedometer    | 1     | —                    | 20 Hz                        |
| Van            | HD Map         | 1     | —                    | OpenDRIVE, static            |

Table 10. **Overview of vehicle sensor configurations.** Abbreviations: F = front, B = back, L = left, R = right, FR = front-right, FL = front-left, RR = rear-right, RL = rear-left, LRR = long-range radar, MRR = mid-range radar.

| Scenario            | Sensor Type    | Count | Position(s) | Resolution / Specs   |
|---------------------|----------------|-------|-------------|----------------------|
| Abandoned Park      | RGB Camera     | 4     | F, B, L, R  | 640×480 px, FOV 90°  |
|                     | Depth Camera   | 1     | F           | 640×480 px, FOV 90°  |
| Africa Savannah     | RGB Camera     | 2     | F, D        | 640×480 px, FOV 90°  |
|                     | Depth Camera   | 1     | F           | 640×480 px, FOV 90°  |
| AirSim NH           | RGB Camera     | 4     | F, L, R, D  | 640×480 px, FOV 90°  |
|                     | Depth Camera   | 1     | F           | 640×480 px, FOV 90°  |
| Landscape Mountains | RGB Camera     | 1     | D           | 640×480 px, FOV 90°  |
|                     | Fisheye Camera | 1     | F           | 640×480 px, FOV 160° |
|                     | Depth Camera   | 1     | F           | 640×480 px, FOV 90°  |
| MS Build 2018       | RGB Camera     | 2     | F, D        | 640×480 px, FOV 90°  |
|                     | Depth Camera   | 1     | F           | 640×480 px, FOV 90°  |

Table 11. **Overview of UAV sensor configurations.** Abbreviations: F = front, B = back, L = left, R = right, D = down.

scenario consistency and tests the agent’s ability to maintain stable perception and control under diverse environmental dynamics.

### 7.3. Manipulation Agent Setups

Following the protocol established in RLBench [33], we evaluate across three available robotic manipulator configurations that are interchanged throughout scenarios: (1) Franka Panda arm with seven joints and the Franka gripper, (2) Sawyer arm with seven joints and Baxter gripper, and (3) UR5 arm with six joints and Robotiq 85 gripper (cf. Figure 4). This multi-embodiment setup ensures broad coverage of kinematic and end-effector characteristics, enhancing the generalizability of our findings.

Beyond ensuring diversity, this design enables us to explicitly evaluate embodiment generalization: rather than

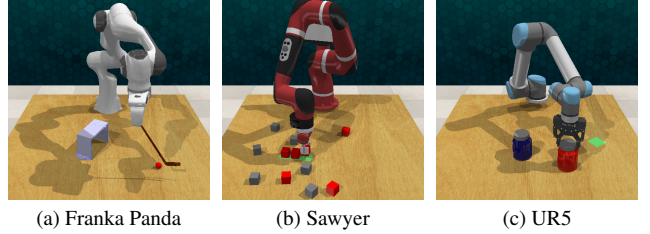


Figure 4. **Illustrative overview of manipulation robotic arm configurations** across the Franka Panda, Sawyer, and UR5 arm.

specializing to a single robot, models must operate consistently across heterogeneous manipulators without retraining or structural modification. This setup reflects the broader goal of embodiment- and sensor-agnostic reasoning, i.e., testing whether a single model can seamlessly handle different embodiments within a shared domain.

## 8. Details of VLN

The VLN component of Embodied4C evaluates how effectively models translate natural language instructions into embodied control actions across three domains: autonomous driving, aerial navigation, and robotic manipulation. Each sub-benchmark follows a consistent scoring and execution framework to ensure comparability across embodiments.

Across all three VLN sub-benchmarks, each episode is executed under a unified timeout protocol that ensures comparability and fairness across embodiments. Timeout durations are adjusted to the embodiment’s physical scale and task complexity: 60–300 s for autonomous driving, 60–180 s for UAV navigation (depending on mission length), and 60–120 s for robotic manipulation. To ensure fair evaluation, the timeout criterion is bound to the actual execution time, excluding latency introduced by VLM inference. Upon timeout, the current binary or graded progress score is reported as the final outcome, preserving diagnostic resolution while preventing reward inflation through excessive deliberation.

### 8.1. Autonomous Driving

In the driving sub-benchmark, simple control tasks are evaluated using a binary scoring scheme, yielding either 0 or 100 points depending on correct execution. More complex tasks are scored using a graded distance-based scheme with a maximum of 50 points, rewarding partial progress towards the target location. A full score of 100 points is assigned if the vehicle satisfies the target criterion  $\Theta$  with additional constraints where applicable. This combination of binary and graded scoring reflects both discrete control actions and spatially precise maneuvers.

We define four scenario categories that reflect increasing complexity of language-guided control tasks:

- **(D1) Basic Control:** Simple binary tasks involving single-step actions such as *HandbrakeLowbeam* or *SteeringSequence*. Success is evaluated with a 0/100 binary criterion (cf. Eq. 5).
- **(D2) Goal-Directed Navigation:** Scenarios such as *Parking*, *TurnLeft*, or *LeaveHighway* require reaching a target location with specific spatial and kinematic tolerances. Here, the 100-point threshold typically combines a distance tolerance  $\epsilon$  (e.g., 1.5–5 m) towards the target location with a speed requirement (e.g.,  $v \leq 0.1 \text{ m/s}$ ) and, where applicable, a lane ID check to ensure correct lane placement (cf. Eq. 6).
- **(D3) Trajectory Following:** Scenarios such as *FollowLane*, *EasySafeDrive*, or *FollowVehicle* evaluate the agent’s ability to follow a reference trajectory or another vehicle over longer distances. 100 points are awarded if a minimum driving distance  $d$  (e.g.,  $d \geq 200 \text{ m}$ ) is achieved while obeying traffic rules. Graded scoring is applied if the target distance is not fully reached (cf. Eq. 6).
- **(D4) Dynamic Interaction.** These scenarios involve more complex temporal coordination with other actors. In the *SpeedLimit* task, Equation 6 is adapted from distance-based to time-based graded scoring, as successful completion requires maintaining a specified speed range for  $t = 10 \text{ s}$ . For *Overtake*, a sequential scoring scheme is applied, assigning partial scores for correctly executed sub-goals in order ((1) Maintain position in the same lane within 20 m of the leading vehicle (+10 pts); (2) Switch to the left lane without collisions or lane invasions. (+20 pts); (3) Pass the leader on the left lane. (+30 pts); (4) Return to the original lane ahead of the leader. (+40 pts)).

Across all scenarios that use graded scoring, common safety termination conditions are enforced. These include **red light violations**, **lane invasions**, and **collisions**. If any of these occur, the scenario is immediately terminated and the score accumulated up to that point is reported. This ensures that unsafe behaviors are penalized while preserving diagnostic resolution. Table 12 lists all driving VLN scenarios, their associated scoring schemes, and the thresholds applied. Scenario names below refer to the naming of scenarios in the code to be released upon publication.

## 8.2. Aerial Navigation

The aerial sub-benchmark follows the same scoring principles but adapts them to the UAV action space. It comprises three scenario categories of increasing instruction and task complexity, progressing from fundamental control understanding to full mission-level flight execution:

- **(A1) Basic Control:** These tasks assess the UAV’s fundamental control understanding through targeted single-

| ID   | Scenario             | Category | Binary | Graded; $\Theta$   |
|------|----------------------|----------|--------|--|
| D1.1 | HandbrakeLowbeam     | D1       | ✓      | –  |
| D1.2 | SteeringSequence     | D1       | ✓      | –  |
| D1.3 | Accelerate           | D1       | ✓      | –  |
| D1.4 | MaintainSpeed        | D1       | ✓      | –  |
| D1.5 | DistanceStop         | D1       | ✓      | –  |
| D2.1 | Parking              | D2       | –      | $\epsilon \leq 1.5 \text{ m} \wedge v \leq 0.1 \text{ m/s}$                    |
| D2.2 | ClearIntersection    | D2       | –      | $\epsilon \leq 5 \text{ m} \wedge v \leq 0.1 \text{ m/s} \wedge \text{laneID}$ |
| D2.3 | Roundabout           | D2       | –      | $\epsilon \leq 5 \text{ m} \wedge \text{laneID}$                               |
| D2.4 | TurnLeft             | D2       | –      | $\epsilon \leq 5 \text{ m} \wedge \text{laneID}$                               |
| D2.5 | LeaveHighway         | D2       | –      | $\epsilon \leq 5 \text{ m} \wedge \text{laneID}$                               |
| D3.1 | EasySafeDrive        | D3       | –      | $d \geq 200 \text{ m}$   |
| D3.2 | FollowLane           | D3       | –      | $d \geq 210 \text{ m} \wedge \text{laneID}$                                    |
| D3.3 | FollowVehicle        | D3       | –      | $\epsilon \leq 15 \text{ m} \wedge d \geq 100 \text{ m}$                       |
| D3.4 | FollowVaryingVehicle | D3       | –      | $\epsilon \leq 20 \text{ m} \wedge d \geq 150 \text{ m}$                       |
| D4.1 | SpeedLimit           | D4       | –      | $t \geq 10 \text{ s} \wedge 80 \leq v \leq 90 \text{ kph}$                     |
| D4.2 | Overtake             | D4       | –      | see Section 8.1  |

Table 12. **Autonomous driving VLN scenarios** with corresponding scoring schemes and thresholds.  $\Theta$  denotes the 100-points target condition if not scored binary.

axis maneuvers (e.g., “*descend 3.2 m*”). A1 scenarios are varied in both action direction and magnitude within the UAV’s control space. Each task includes a single success condition, evaluated using binary 0/100 scoring (cf. Eq. 5).

- **(A2) Goal-Directed Navigation:** Goal-directed navigation tasks require the UAV to execute compound flight sequences that jointly control altitude, orientation, and translation (e.g., “*ascend 12 m, turn 70° left, and continue straight for 10 m while maintaining altitude*”). Each sequence implicitly defines a spatial goal state in 3D airspace relative to the UAV’s initial position  $d_{\text{init}}$ . Progress is evaluated through a graded scoring scheme that computes the Euclidean distance between the UAV’s final and target positions  $d_{\text{agt}}$ , normalized with respect to  $d_{\text{init}}$ , linearly distributing up to 50 points across this range until the UAV reaches the 100-point termination threshold (cf. Eq. 6). A perfect score of 100 is assigned when the UAV terminates within  $\theta_{\text{agt}} \leq 1 \text{ m}$  of the aerial target, reflecting the required spatial precision for controlled flight trajectories. To further encourage correct directional progress throughout the episode, the scoring is extended to continuously record the minimum achieved distance to the target,  $d_{\text{min}}$ . The similar graded function is applied to this distance, producing a maximum progress score that rewards movement toward the correct aerial direction, even if the UAV overshoots the target. The final score is computed as a weighted combination of the terminal distance score and the maximum progress score, prioritizing successful goal completion (90%) while maintaining sensitivity to directional accuracy (10%).

- **(A3) Mission-level Execution:** These scenarios involve complex, high-level flight missions that demand coordinated spatial reasoning and temporal consistency, such as “*LandInMiddleCircle*” or “*HoverAboveCrocodile*”. Since mission completion either fails or succeeds, binary 0/100 scoring is applied (cf. Eq. 5). Partial progress

| ID        | Scenario                 | Category | Binary | Graded; $\Theta$   |
|-----------|--------------------------|----------|--------|--|
| A1.1-1.4  | SingleControlAction (x4) | A1       | ✓      | —  |
| A2.1-2.12 | ControlSequence (x12)    | A2       | —      | $\epsilon \leq 1 \text{ m}$                                      |
| A3.1      | FlyToMerryGoAround       | A3       | ✓      | $\epsilon \leq 5 \text{ m} \wedge  \delta_h  \leq 1 \text{ m}$   |
| A3.2      | LandInMiddleCircle       | A3       | ✓      | $\epsilon \leq 10 \text{ m} \wedge  \delta_h  \leq 1 \text{ m}$  |
| A3.3      | LandOnRefereeShelter     | A3       | ✓      | $\epsilon \leq 3.5 \text{ m} \wedge  \delta_h  \leq 1 \text{ m}$ |
| A3.4      | HoverAboveCrocodile      | A3       | ✓      | $\epsilon \leq 4 \text{ m} \wedge  \delta_h  \leq 1 \text{ m}$   |
| A3.5      | LandOnTrashCan           | A3       | ✓      | $\epsilon \leq 1.5 \text{ m} \wedge  \delta_h  \leq 1 \text{ m}$ |
| A3.6      | SearchTunnelEntrance     | A3       | ✓      | $\epsilon \leq 15 \text{ m} \wedge  \delta_h  \leq 1 \text{ m}$  |

Table 13. **Aerial navigation VLN scenarios** with corresponding scoring schemes and thresholds.  $\Theta$  denotes the 100-points target condition.

is not rewarded, as incomplete execution typically violates the mission objective or safety constraints inherent to UAV operation. A scenario-specific target region defines successful completion, with thresholds detailed in Table 13. To ensure accurate vertical positioning, an additional altitude constraint  $\delta_h$  is enforced, with  $|\delta_h| \leq 1 \text{ m}$ . Exceeding this tolerance results in mission failure and a score of 0.

### 8.3. Robotic Manipulation

The manipulation sub-benchmark defines three scenario categories reflecting increasing complexity in language-guided robotic control. Table 14 lists all scenarios, their categories, and associated scoring schemes.

- **(M1) Basic Control:** These are simple, single-step tasks involving the actuation of a single joint or the gripper (e.g., *open/close gripper*, *move one joint*). Each M1 scenario is randomly varied within the robot’s action space, but only a single action is required for success. Success is evaluated using a binary 0/100 criterion (cf. Eq. 5).
- **(M2) Goal-Directed Navigation:** These tasks involve multi-step, sequence-based navigation of the end-effector (e.g., *“move 30 cm forward, then 30 cm right, then 30 cm down”*). Each sequence is randomly shuffled along the three orthogonal axes, so that while the distances remain fixed at 30 cm per step, the order of the directions and end target location varies. Graded scoring is applied: partial credit of up to 50 points is awarded based on the reduction of the initial distance to the target ( $d_{\text{init}} = 51.9 \text{ cm}$ ), and full 100 points are granted only if the agent reaches within  $\theta_{\text{agt}} \leq 2.5 \text{ cm}$  of the goal (cf. Eq. 6). This strict tolerance reflects the high precision required for manipulation, where even small deviations can prevent task success.
- **(M3) Dynamic Interaction:** Complex tasks such as *BasketballInHoop*, *PushButtons*, and *OpenJar* demand precise, sequential coordination to achieve a defined goal. Since each task represents a single, well-defined mission (e.g., the ball either lands in the hoop or not), outcomes are evaluated using a binary 0/100 score (cf. Eq. 5). Partial progress is not rewarded, as success depends on completing the full objective.

| ID        | Scenario                 | Category | Binary | Graded; $\Theta$               |
|-----------|--------------------------|----------|--------|--------------------------------|
| M1.1-1.2  | SingleControlAction (x2) | M1       | ✓      | —                              |
| M2.1-2.12 | ControlSequence (x12)    | M2       | —      | $\epsilon \leq 2.5 \text{ cm}$ |
| M3.1      | BasketballInHoop         | M3       | ✓      | —                              |
| M3.2      | PutRubbishInBin          | M3       | ✓      | —                              |
| M3.3      | CloseLaptopLid           | M3       | ✓      | —                              |
| M3.4      | PushButtons              | M3       | ✓      | —                              |
| M3.5      | OpenJar                  | M3       | ✓      | —                              |
| M3.6      | ReachTarget              | M3       | ✓      | —                              |

Table 14. **Robotic manipulation VLN scenarios** with corresponding scoring schemes and thresholds.  $\Theta$  denotes the 100-points target condition.

## 9. Autonomous Agent Models

### 9.1. Driving Agent Models

We select **Senna** [34] as our driving baseline model due to its combination of open-source availability (OSA: ✓), and its support for interactive VQA, VLN, and spatial understanding. While models like DriveVLM [77] and Open-DriveVLA [104] offer advanced reasoning or multimodal fusion, they lack accessible code or inference pipelines (cf. Table 15). Senna’s public implementation enables reproducible evaluation of interactive driving.

**Senna** is a composite vision-language driving model in which the core decision-making logic is realized by Senna-VLM. The backbone of Senna-VLM is based on Vicuna-7B-v1.5 following the LLaVA architecture paradigm, where a vision encoder is coupled to the language model through a *driving-specific multimodal adapter*. This design enables Senna-VLM to generate structured natural language outputs that articulate driving intent and scene interpretation. Senna operates on a fixed surround-view camera configuration of six images to maintain global spatial awareness. The model assumes this input dimensionality as part of its internal feature alignment; deviations from this requirement lead to inference failure. To accommodate varying real-world sensor setups of Embodied4C, we enforce a strict input normalization step: if fewer than six views are available, a placeholder (dummy) frame is inserted, and if more than six are present, the input is truncated. All experiments are conducted with Senna in 4-bit precision.

### 9.2. UAV Agent Models

We adopt **OpenFly-Agent** [22] as the UAV baseline. Among current models (cf. Table 16), it is one of the few that is fully open-source (OSA: ✓) and publicly released on Hugging Face, enabling transparent and reproducible evaluation. In contrast, most UAV VLN models either lack released checkpoints, rely on proprietary training pipelines, or provide perception-only components without actionable control policies.

**OpenFly-Agent** integrates a visual encoder with a LLaMA-derived language model and outputs a 6-

| Model                   | SEM | SPA | TEM | PHY | INT | VLN | OSA |
|-------------------------|-----|-----|-----|-----|-----|-----|-----|
| LanguageMPC [67]        | ✗   | ✗   | ✗   | ✗   | ✗   | ✗   | ✗   |
| DME-Driver [26]         | ✗   | ✓   | ✗   | ✗   | ✗   | ✗   | ✗   |
| VLM-AD [90]             | ✗   | ✗   | ✓   | ✗   | ✗   | ✗   | ✗   |
| GPT-Drive [49]          | ✗   | ✗   | ✗   | ✗   | ✗   | ✗   | ✓   |
| OpenEMMA [89]           | ✗   | ✗   | ✗   | ✗   | ✗   | ✗   | ✓   |
| LightEMMA [60]          | ✗   | ✗   | ✗   | ✗   | ✗   | ✗   | ✓   |
| EMMA [30]               | ✗   | ✗   | ✗   | ✗   | ✓   | ✗   | ✗   |
| Reason2Drive [53]       | ✗   | ✗   | ✗   | ✗   | ✓   | ✗   | ✗   |
| DriveVLM [77]           | ✗   | ✗   | ✗   | ✗   | ✓   | ✗   | ✗   |
| InternVLM-Drive-v2 [42] | ✗   | ✗   | ✓   | ✗   | ✓   | ✗   | ✗   |
| LaVida-Drive [35]       | ✗   | ✓   | ✓   | ✗   | ✓   | ✗   | ✗   |
| BEV-InMLLM [15]         | ✗   | ✓   | ✓   | ✗   | ✓   | ✗   | ✗   |
| LiDAR-LLM [93]          | ✗   | ✓   | ✗   | ✗   | ✓   | ✗   | ✗   |
| OpenDriveVLA [104]      | ✓   | ✓   | ✗   | ✗   | ✓   | ✗   | ✗   |
| OcclLlaMA [83]          | ✓   | ✓   | ✓   | ✗   | ✓   | ✗   | ✗   |
| DriverAgent [36]        | ✗   | ✗   | ✗   | ✗   | ✗   | ✓   | ✗   |
| CarLlaVA [62]           | ✗   | ✗   | ✗   | ✗   | ✗   | ✓   | ✗   |
| HE-Drive [79]           | ✗   | ✗   | ✗   | ✗   | ✓   | ✗   | ✓   |
| RDA-Drive [29]          | ✗   | ✗   | ✗   | ✗   | ✓   | ✗   | ✓   |
| LLM-Drive [10]          | ✗   | ✗   | ✗   | ✗   | ✓   | ✗   | ✓   |
| DriveMM [28]            | ✗   | ✗   | ✗   | ✗   | ✓   | ✗   | ✓   |
| DriveLM-Agent [71]      | ✗   | ✗   | ✗   | ✗   | ✓   | ✗   | ✓   |
| RAG-Drive [96]          | ✗   | ✗   | ✗   | ✗   | ✓   | ✗   | ✓   |
| BeVLM [17]              | ✗   | ✓   | ✗   | ✗   | ✓   | ✗   | ✓   |
| Dolphins [48]           | ✓   | ✓   | ✗   | ✓   | ✓   | ✗   | ✓   |
| DriveGPT4 [91]          | ✗   | ✓   | ✓   | ✗   | ✓   | ✗   | ✓   |
| OmniDrive-Agent [80]    | ✗   | ✓   | ✓   | ✗   | ✓   | ✗   | ✓   |
| ELM [105]               | ✗   | ✓   | ✓   | ✗   | ✓   | ✗   | ✓   |
| LMDrive [69]            | ✗   | ✗   | ✗   | ✗   | ✗   | ✓   | ✓   |
| Agent-Drive [50]        | ✗   | ✗   | ✗   | ✗   | ✗   | ✓   | ✓   |
| DriveMLM [81]           | ✗   | ✗   | ✗   | ✗   | ✓   | ✓   | ✗   |
| ORION [20]              | ✗   | ✗   | ✓   | ✗   | ✓   | ✓   | ✗   |
| Senna [34]              | ✗   | ✓   | ✗   | ✗   | ✓   | ✓   | ✓   |
| SimLingo [63]           | ✗   | ✓   | ✗   | ✗   | ✓   | ✓   | ✓   |
| AsyncDriver [11]        | ✓   | ✗   | ✗   | ✗   | ✓   | ✓   | ✓   |

Table 15. **Overview of state-of-the-art driving agent models.** Columns “SEM”, “SPA”, “TEM”, and “PHY” indicate the inclusion of semantic, spatial, temporal, and physical understanding. “INT” and “VLN” denote support for interaction through VQA and vision-language navigation, while “OSA” marks open source availability (as of August 2025).

dimensional action vector:

[forward, turn\_left, turn\_right, move\_up, move\_down, stop],

where each action corresponds to a fixed displacement of 3 m or a rotation step of 30°. For VLN tasks, we map these commands to the unified low-level control interface of each sub-benchmark, ensuring consistent actuation across agent setups. For VQA tasks, OpenFly’s action head is bypassed to force textual responses, supported by an additional, minimal system instruction that enforces concise English output. Since the language model backbone was trained solely for action vector generation, it produces nonsensical text outputs, yielding zero scores (cf. Section 4). All experiments are conducted with Open-Fly Agent in 4-bit precision.

### 9.3. Manipulation Agent Models

For manipulation tasks, we adopt two open-source VLA baselines: **OpenVLA** [37] and **MolmoAct** [39], both available through public checkpoints (OSA: ✓) and thus suit-

| Model               | SEM | SPA | TEM | PHY | INT | VLN | OSA |
|---------------------|-----|-----|-----|-----|-----|-----|-----|
| CognitiveDrone [47] | ✓   | ✗   | ✗   | ✗   | ✗   | ✓   | ✗   |
| LogisticsVLM [99]   | ✓   | ✓   | ✗   | ✗   | ✗   | ✓   | ✗   |
| VLFly [100]         | ✓   | ✓   | ✗   | ✗   | ✗   | ✓   | ✗   |
| UAV-VLM [66]        | ✓   | ✓   | ✗   | ✗   | ✗   | ✓   | ✗   |
| UAV-VLA [65]        | ✓   | ✓   | ✗   | ✗   | ✗   | ✗   | ✓   |
| LAG [45]            | ✓   | ✓   | ✗   | ✗   | ✗   | ✓   | ✓   |
| OpenFly-Agent [22]  | ✓   | ✓   | ✓   | ✗   | ✗   | ✓   | ✓   |

Table 16. **Overview of state-of-the-art UAV agent models.** Columns “SEM”, “SPA”, “TEM”, and “PHY” indicate the inclusion of semantic, spatial, temporal, and physical understanding. “INT” and “VLN” denote support for interaction through VQA and vision-language navigation, while “OSA” marks open source availability (as of September 2025).

able for reproducible, controlled comparison (cf. Table 17). Closed-source systems, such as LA-RCS [58] and RT-2 [106], are excluded due to deployment limitations.

**OpenVLA** is trained on large-scale robotic demonstration datasets and predicts continuous 7-DoF control commands for end-effector translation ( $\Delta x, \Delta y, \Delta z$ ), rotation ( $\Delta \alpha, \Delta \beta, \Delta \gamma$ ), and gripper state  $g$ . To ensure consistent execution across our sub-benchmark environments, we map these outputs into the standardized control interface and apply scaling adjustment. For VQA-style tasks, the action head is bypassed, and the language component is prompted directly to produce concise English answers using a minimal instruction. However, since the language backbone was trained solely for action prediction, direct text decoding produces nonsensical outputs, resulting in uniform zero scores. All experiments are conducted with OpenVLA in 4-bit precision. **MolmoAct** similarly provides a 7-DoF action head but supports explicit switching between action prediction and text generation. We use the MolmoAct-7B-D-0812 release and provide an additional alignment prompt to standardize its action dimensions to corresponding sub-benchmark interfaces. For VQA tasks, we directly decode language tokens, while VLN tasks use the native action outputs.

This setup allows consistent cross-model comparison of scenario understanding among the four capability dimensions and action execution.

## 10. Additional Results

### 10.1. Sub-Capability Analysis

The heatmap summarizes performance across the 18 sub-capabilities of Embodied4C and the generalization category (GEN). Horizontally (across models), a clear scaling trend emerges: large frontier models (GPT-5 [54], Claude Sonnet 4.5 [1], LLaMA 4 Maverick [52]) achieve substantially higher average performance, while smaller models ( $\leq 7B$ ) show consistently lower scores. Domain-specialized embodied agents fail significantly across all sub-capabilities,

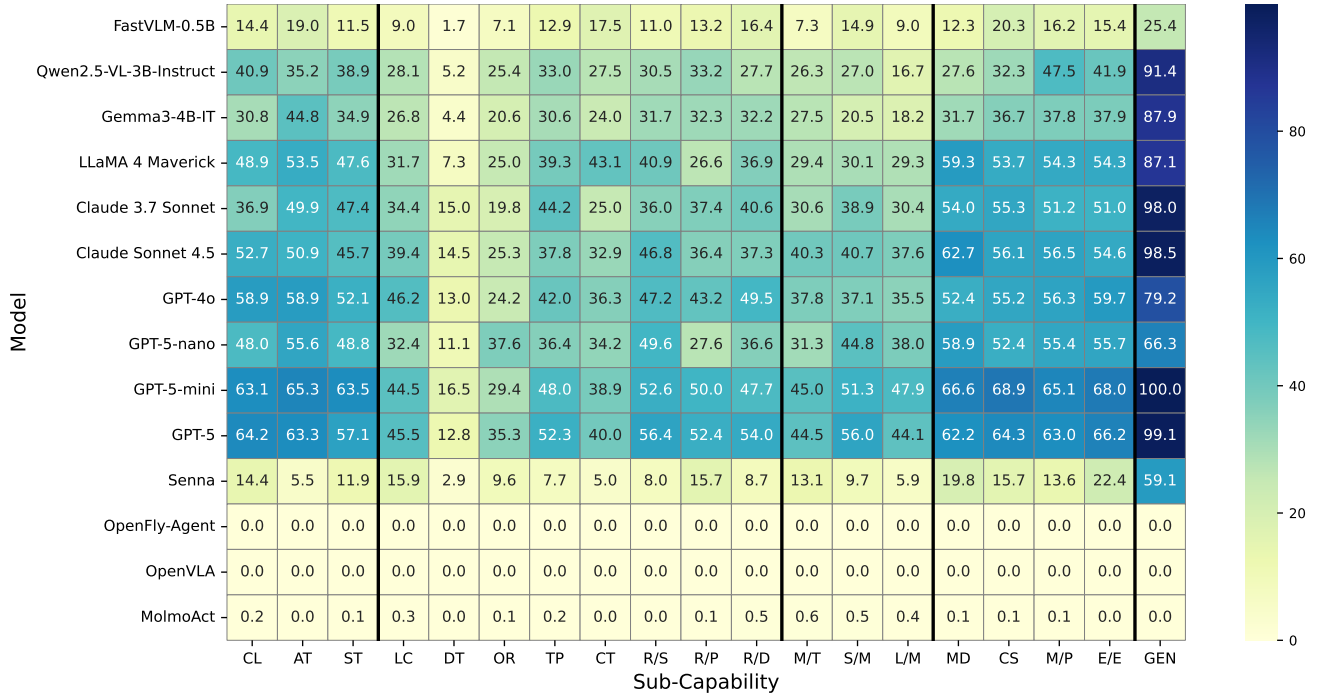


Figure 5. **Per-model performance across fine-grained sub-capabilities in the Embodied4C benchmark.** Each cell shows the mean accuracy (%) for a model (rows) on a sub-capability (columns). Sub-capabilities are grouped into main capabilities (separated by thick vertical lines): semantic (CL, AT, ST), spatial (LC, DT, OR, TP, CT), temporal Reasoning (R/S, R/P, R/D), and physical reasoning (M/T, S/M, L/M, MD, CS, M/P, E/E). The final column (GEN) reports performance on general knowledge questions.

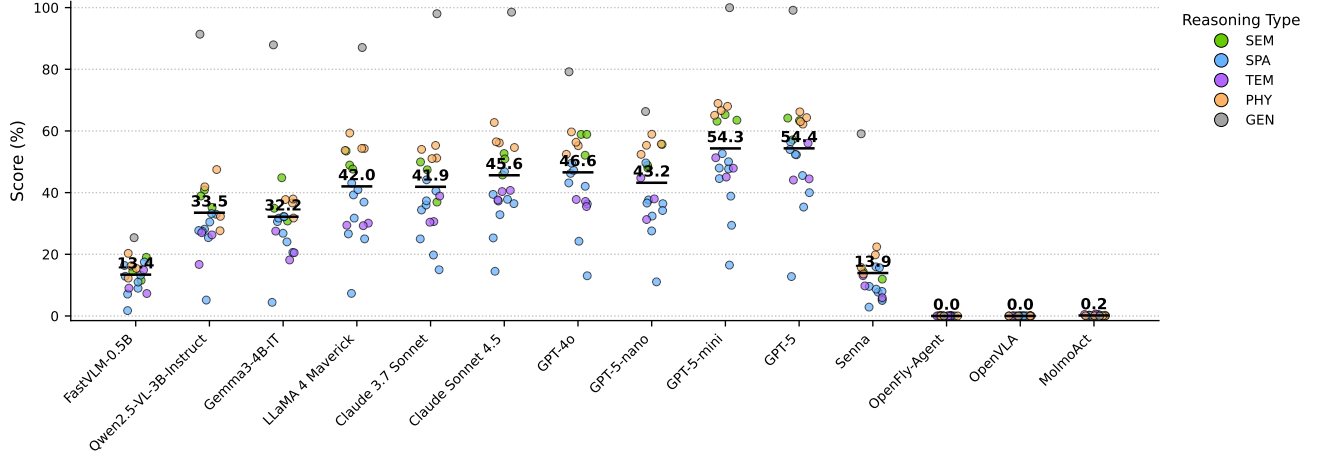


Figure 6. **Model robustness across Embodied4C sub-capabilities.** Each dot represents a model's mean score on one sub-capability (19 total), jittered horizontally for clarity; the black bar marks the model's overall VQA mean. Color encodes high-level reasoning type: semantic, spatial, temporal, physical, and generalization.

as training distributions and bypassing their action heads yields bad or no coherent language output.

as:

$$CV = \frac{\sigma}{\mu}, \quad CV\% = 100 \cdot \frac{\sigma}{\mu}, \quad (10)$$

To further characterize cross-capability stability (cf. Figure 6), we analyze the coefficient of variation (CV), defined

where  $\mu$  is the mean performance over sub-capabilities and  $\sigma$  is the standard deviation. CV provides a scale-normalized

| Model           | SEM | SPA | TEM | PHY | INT | VLN | OSA |
|-----------------|-----|-----|-----|-----|-----|-----|-----|
| MALMM [72]      | ✓   | ✓   | ✗   | ✗   | ✗   | ✓   | ✗   |
| LA-RCS [58]     | ✓   | ✓   | ✓   | ✗   | ✓   | ✓   | ✗   |
| RT-2 [106]      | ✓   | ✓   | ✗   | ✓   | ✓   | ✓   | ✗   |
| CLIPort [70]    | ✓   | ✓   | ✗   | ✗   | ✗   | ✓   | ✓   |
| VoxPoser [27]   | ✓   | ✓   | ✗   | ✗   | ✗   | ✓   | ✓   |
| RT-1 [6]        | ✓   | ✓   | ✗   | ✗   | ✗   | ✓   | ✓   |
| SpatialVLA [61] | ✓   | ✓   | ✗   | ✗   | ✗   | ✓   | ✓   |
| OpenVLA [37]    | ✓   | ✓   | ✗   | ✗   | ✗   | ✓   | ✓   |
| MolmoAct [39]   | ✓   | ✓   | ✗   | ✗   | ✗   | ✓   | ✓   |

Table 17. **Overview of state-of-the-art manipulation agent models.** Columns “SEM”, “SPA”, “TEM”, and “PHY” indicate the inclusion of semantic, spatial, temporal, and physical understanding. “INT” and “VLN” denote support for interaction through VQA and vision-language navigation, while “OSA” marks open source availability (as of September 2025).

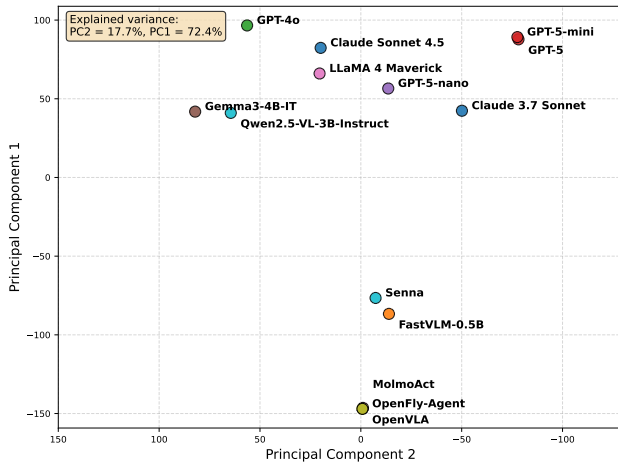


Figure 7. **Principle component analysis of Embodied4C model capability profiles.** PC1 (72.4%) reflects overall embodied competence, separating low-level visuomotor models from high-capability multimodal reasoners. PC2 (17.7%) distinguishes reasoning strategy, ranging from language-driven planning to direct perception-to-action control.

measure of dispersion, enabling fair comparison between models with different absolute score ranges. Smaller models (e.g., Qwen2.5-VL-3B-Instruct [3], Gemma3-4B-IT [23]) exhibit high variability ( $CV \approx 50\%$ ), indicating inconsistent reasoning capabilities across the capability spectrum. In contrast, higher-capability frontier models demonstrate more stable behavior: GPT-5 achieves  $\mu = 54.4$ ,  $\sigma = 16.9$ ,  $CV = 31.1\%$ , and GPT-4o [75] similarly maintains lower dispersion ( $CV = 31.3\%$ ). This trend suggests that scaling not only improves average capability but also reduces cross-capability unevenness.

Vertically (across sub-capabilities), two clusters emerge. *Spatial* and *Physical* reasoning are comparatively stronger (up to 68.9%), particularly for model dynamics

(MD) and environmental effects (E/E). Conversely, *Spatial* and *Temporal* reasoning remain major failure modes. Distance estimation (DT) is the weakest dimension overall ( $\mu = 7.46$ ), followed by orientation (OR) and counting (CT); within *Temporal*, short-term memory (S/M) outperforms movement-time (M/T) and long-term memory (L/M), but all remain low.

Finally, generalization (GEN) is near-saturated for the strongest models, reflecting robustness to domain-far linguistic variation. Notable deviations (e.g., GPT-4o scoring lower despite strong average performance) suggest sensitivity to distractors or prompt instability rather than inability to generalize. Table 18 provides additional statistical features across all tested models.

## 10.2. Principal Component Analysis

To understand the latent structure underlying model behavior in Embodied4C, we perform a PCA over model-level capability vectors spanning semantic, spatial, temporal, and physical reasoning across all embodied domains. The resulting projection identifies two orthogonal dimensions—PC1 and PC2—that together explain **90.1%** of the total variance (72.4% and 17.7%, respectively). These components reveal not only performance magnitude but also distinct strategies through which embodied reasoning competence emerges.

**PC1: Overall Benchmarked Performance.** The first principal component reflects a near-linear correlation with the overall **E4C-S** score and the averaged domain scores (DS, AS, MS). Models with high PC1 values—most notably GPT-5-mini, GPT-5, and Claude Sonnet 4.5—exhibit the strongest integrated performance across all embodied domains, achieving the top E4C-S values of **39.59**, **36.00**, and **31.78**, respectively. In contrast, models such as Senna, OpenVLA, and MolmoAct cluster at the negative end of PC1 with E4C-S scores below **8.5**, indicating poor general reasoning and limited cross-modal transfer. PC1 thus quantifies *global embodied competence*, representing the dominant axis of model performance variation across the benchmark.

**PC2: Generality and Robustness vs. Core VQA Capability.** The second component captures an orthogonal dimension that differentiates models by their *strategy of achieving high performance*. It contrasts robustness and generalization strength against specialization in core VQA sub-capabilities. Negative PC2 values correspond to models exhibiting **high generality and robustness**—notably GPT-5 and GPT-5-mini, both scoring near-perfect on the Domain-far QA metric ( $\approx 100\%$ ). Their performance reflects stable reasoning across unfamiliar scenarios and minimal overfitting. Positive PC2 values are associated with

| Model                      | Mean | Std  | Min  | Max   | Range | CV%    | # > 0 |
|----------------------------|------|------|------|-------|-------|--------|-------|
| FastVLM-0.5B [38]          | 13.4 | 5.4  | 1.7  | 25.4  | 23.7  | 40.4%  | 19    |
| Qwen2.5-VL-3B-Instruct [3] | 33.5 | 16.8 | 5.2  | 91.4  | 86.2  | 50.2%  | 19    |
| Gemma3-4B-IT [23]          | 32.2 | 16.2 | 4.4  | 87.9  | 83.5  | 50.3%  | 19    |
| LLaMA 4 Maverick [52]      | 42.0 | 17.2 | 7.3  | 87.1  | 79.7  | 40.9%  | 19    |
| Claude 3.7 Sonnet [2]      | 41.9 | 17.7 | 15.0 | 98.0  | 83.0  | 42.3%  | 19    |
| Claude Sonnet 4.5 [1]      | 45.6 | 17.3 | 14.5 | 98.5  | 84.0  | 37.9%  | 19    |
| GPT-4o [75]                | 46.6 | 14.6 | 13.0 | 79.2  | 66.1  | 31.3%  | 19    |
| GPT-5-nano [54]            | 43.2 | 13.3 | 11.1 | 66.3  | 55.2  | 30.8%  | 19    |
| GPT-5-mini [54]            | 54.3 | 17.7 | 16.5 | 100.0 | 83.5  | 32.6%  | 19    |
| GPT-5 [54]                 | 54.4 | 16.9 | 12.8 | 99.1  | 86.4  | 31.1%  | 19    |
| Senna [34]                 | 13.9 | 12.1 | 2.9  | 59.1  | 56.2  | 86.9%  | 19    |
| OpenFly-Agent [22]         | 0.0  | 0.0  | 0.0  | 0.0   | 0.0   | –      | 0     |
| OpenVLA [37]               | 0.0  | 0.0  | 0.0  | 0.0   | 0.0   | –      | 0     |
| MolmoAct [39]              | 0.2  | 0.2  | 0.0  | 0.6   | 0.6   | 115.8% | 17    |

Table 18. **Per-model VQA performance across 19 sub-capabilities in Embodied4C.** Reported statistics (mean, standard deviation, min, max, range, coefficient of variation, and count of non-zero scores) summarize accuracy scores (0–100%) over fine-grained scenario understanding capabilities and tasks spanning autonomous driving, UAV navigation, and robotic manipulation.

models whose strength lies in **core visuolinguistic reasoning**, such as GPT-4o, Claude Sonnet 4.5, Gemma3-4B-IT, and Qwen2.5-VL, which achieve high spatial and temporal understanding but lower generalization. Importantly, this axis must be interpreted *relative to overall capability (PC1)*: models with low E4C-S, such as Senna, may appear in the positive PC2 range due to unbalanced or noisy sub-capability patterns rather than genuine VQA specialization. PC2 therefore encodes a *trade-off axis between generality and VQA specialization*, meaningful primarily when considered in conjunction with global competence along PC1.

**Interpretation.** The two principal components together delineate a coherent performance manifold across embodied foundation models.

- The **upper region (high PC1)** corresponds to globally strong performers with well-integrated multimodal reasoning.
- The **left side (low PC2)** identifies the most general and robust models (relative to PC1), resilient to domain shifts and linguistic perturbations.
- The **right side (high PC2)** captures models whose strength lies in precise, domain-specific VQA competence.
- Finally, the **bottom region (low PC1)** groups weakly capable VLA models dominated by sensorimotor coupling without transferable reasoning.

In summary, PC1 measures the *depth* of embodied reasoning, while PC2 measures its *robustness–specialization trade-off*. The top-right quadrant, occupied by GPT-5 and GPT-5-mini, marks the region of **maximal embodied general intelligence**: high overall competence, balanced multimodal understanding, and robust generalization across domains.